Evolution of the eyes of vipers with and without infrared-sensing pit organs

David J. Gower[1,*], Filipa L. Sampaio[1], Leo Peichl[2,3], Hans-Joachim Wagner[4], Ellis R. Loew[5], William McLamb[6], Ronald H. Douglas[1,7], Nikolai Orlov[8]; Michael S. Grace[9], Nathan S. Hart[10], David M. Hunt[11,12], Julian C. Partridge[11,13] and Bruno F. Simões[1,14, 15*]

[1] Department of Life Sciences, The Natural History Museum, London, SW7 5BD, UK.
[2] Max Planck Institute for Brain Research, 60438 Frankfurt am Main, Germany
[3] Dr. Senckenbergische Anatomie, Goethe University Frankfurt, Theodor-Stern-Kai 7, 60590 Frankfurt am Main, Germany
[4] Anatomisches Institut, Universität Tübingen, Österbergstr. 3, D-72074 Tübingen, Germany
[5] Department of Biomedical Sciences, Cornell University, Ithaca, New York, 14853, USA
[6] Department of Biological Sciences, Florida Institute of Technology, and Center for the Advancement of Science in Space, Melbourne, Florida, USA
[7] Department of Optometry and Visual Science, City, University of London, London EC1V 0HB, UK
[8] Department of Herpetology, Zoological Institute, Russian Academy of Sciences, Universitetskaya nab. 1, St. Petersburg, 199034, Russia
[9] College of Science, Florida Institute of Technology,
[10] Department of Biological Sciences, Macquarie University, North Ryde, NSW 2109 Australia
[11] School of Biological Sciences, The University of Western Australia, Perth, WA 6009, Australia
[12] Centre for Ophthalmology and Vision Science, Lions Eye Institute, The University of Western Australia, Perth, 6009, Australia
[13] Oceans Institute, The University of Western Australia, Perth, WA 6009, Australia
[14] School of Earth Sciences, University of Bristol, Bristol BS8 1TG, United Kingdom
[15] School of Biological Sciences, University of Adelaide, Adelaide, South Australia 5000, Australia

*Email: bruno.simoes@me.com; d.gower@nhm.ac.uk

Running title: EVOLUTION OF EYES IN VIPERID SNAKES

We examined lens and brille transmittance, photoreceptors, visual pigments, and visual opsin gene sequences of viperid snakes with and without infrared-sensing pit organs. Ocular media transmittance is high in both groups. Contrary to previous reports, small as well as large single cones occur in pit vipers. Non-pit vipers differ from pit vipers in having a two-tiered retina, but few taxa have been examined for this poorly understood feature. All vipers sampled express *rh1, sws1* and *lws* visual opsin genes. Opsin spectral tuning varies but not in accordance with the presence/absence of pit organs, and not always as predicted from gene sequences. The visual opsin genes were generally under purifying selection, with positive selection at spectral tuning amino acids in RH1 and SWS1 opsins, and at retinal pocket stabilization sites in RH1 or LWS (and without substantial differences between pit and non-pit vipers). Lack of evidence for sensory trade-off between viperid eyes (in the aspects examined) and pit organs might be explained by the high degree of neural integration of vision and infrared detection; the latter representing an elaboration of an existing sense with addition of a novel sense organ, rather than involving the evolution of a wholly novel sensory system.

ADDITIONAL KEYWORDS: molecular evolution – ocular media – opsin – photoreceptors – retina – snakes – spectral tuning – Viperidae.

INTRODUCTION

What happens to animals' sensory systems when one system is elaborated or a novel system evolves? This is a topic of substantial interest in sensory and evolutionary biology, and among vertebrates there are several striking instances of new and/or elaborated senses occurring in taxa in which other senses are degenerate. For example, echolocating bats and toothed whales have reduced visual and olfactory systems, respectively (Oelschläger, 1992; Jones, Teeling, & Rossiter, 2013; Hudson *et al.*, 2014); the two trichromatic lineages of primates have a significantly more degenerate olfactory repertoire than other primates (Gilad *et al.*, 2004); the mostly soil-dwelling caecilian amphibians have a reduced visual system but a unique, probably chemosensory and tactile tentacle (Himsted, 1996; Mohun *et al.*, 2010); small-eyed star-nosed moles, naked mole-rats and duck-billed platypuses all have reduced vision and an elaborated somatosensory/electrosensory system (e.g., Pettigrew *et al.*, 1998; Catania & Remple, 2004; Catania, 2011); and cave fish with reduced vision have hypertrophied mechanosensory lateral line systems and enhanced gustatory and possibly olfactory systems (e.g. Soares & Niemiller, 2013). Most, if not all, of these examples, however, can be argued to be cases of elaboration as a compensation for the reduction in the utility of a major sense following a substantial shift from an ancestral ecology. As stated by Zhao et al. (Zhao *et al.*, 2009a) "where sensory losses occur, they are typically associated with a cessation of sensory input rather than via a trade-off per se".

Nevertheless, trade-offs might be expected in sensory system evolution (Niven & Laughlin, 2008) because the relatively high energetic expense of neural tissue makes the unconstrained addition of new sensory modalities extremely unlikely, as evidenced by the limited set of sensory systems observable in any one organism. Not only do the peripheral

sense organs themselves have metabolic demands, but so too do the neural centres required to process sensory inputs. To understand sensory evolution further there is a need to explore possible sensory trade-offs in more "phenotypically and phylogenetically divergent taxa" (Zhao *et al.*, 2009a). The impact of the evolution of infrared (IR) detection in pit vipers may be a good case study, because these snakes use their apomorphic IR detection for several important functions including prey (and possibly predator) detection and thermoregulation (Krochmal, 2004), and their IR imaging sensors are the most sensitive and efficient known (e.g., Grace & Matshita, 2007). Additionally, an inverse relationship has been found between the size of the eyes and the pits in pit vipers (Liu *et al.*, 2016).

Uniquely among the three subfamilies of viperid snakes, crotaline (or pit) vipers possess highly specialized, bilateral facial pit organs that are acutely sensitive to IR radiation (wavelengths of 700 nm to 1 mm). Unlike the sensing of the visual spectrum (ca. 300–800 nm when all animals are considered; ca. 400–700 nm for human vision), which is mediated by photochemical transduction, pit viper IR imaging is achieved by thermotransduction (Gracheva *et al.*, 2010). However, information from the eyes and IR pit organs is integrated neurally in the snakes' central nervous system. In the optic tectum, IR nerve fibres synapse directly with visual neuron dendrites and the visual and IR spatiotopic maps are correlated (Hartline *et al.,* 1978; Newman & Hartline, 1981). Thus, pit vipers construct broad-band images combining visual and thermal radiation (Goris, 2011). As a result, the apomorphic IR sense of pit vipers is well integrated with the animals' visual system to provide spatial vision over a wide range of wavelengths.

Viperid snakes are generally nocturnal, and all are venomous predators of a range of vertebrates and invertebrates. Variation in size, diet and daily activity patterns is not neatly partitioned among the three subfamilies; the 70–210 cm long Old World viperines, ca. 70 cm

southeast Asian azemiopines, and 30–370 cm Eurasian and New World crotalines. The basal divergence between Viperinae and Crotalinae + Azemiopinae has been estimated to have occurred in the Eocene, and the split between Crotalinae and Azemiopinae in the Late Eocene or Oligocene (Wüster *et al.*, 2008; Harrington & Reeder, 2017). The non-crotaline vipers (Viperinae and Azemiopinae) are paraphyletic with respect to Crotalinae and lack IR pit organs. Thus, pit viper IR sensing is probably tens of millions of years old, and the absence of pit organs in azemiopines and viperines is, on the basis of parsimony, presumably plesiomorphic. In addition to the IR pit organs, pit and non-pit vipers seemingly differ in their complement of retinal photoreceptor cells. Viperines are reported to possess four photoreceptor classes (rods, small and large single cones, and double cones), while crotalines have three classes, and lack small single cones (Walls, 1942; Underwood, 1967; Underwood, 1970). The condition in Azemiopinae is not known.

The striking, mutually exclusive taxonomic distribution of small single cones and IR pit organs among different lineages of vipers, and the neural integration of thermo- and photochemical imaging in pit vipers, begs two obvious questions: (1) is vision different in pit and non-pit vipers (in ways other than the presence or absence of small single cones)?, and (2) are the differences attributable to the evolutionary acquisition of IR detection?

Here we explore the impact on aspects of vision of the evolutionary acquisition of IR detection in pit vipers. We undertook an integrative approach combining microspectrophotometry (MSP) to measure visual pigment absorption spectra in situ in single retinal photoreceptors, immunohistochemistry of retinal photoreceptors to identify different cell types by their opsin complement, measurements of spectral transmittance of lenses and brilles to understand the light reaching the retina, histology to examine retinal anatomy, and cDNA sequencing of visual pigment genes to elucidate their evolutionary

history and mechanisms of spectral tuning.

MATERIAL AND METHODS

TAXON AND GENE SAMPLING

The approximately 350 extant viperid species are classified into three subfamilies, the Viperinae (ca. 30% of species), Azemiopinae (only two species), and Crotalinae (70%); Azemiopinae and Crotalinae being sister groups (Cadle, 1992; Wüster *et al.*, 2008). We sampled 13 species (11 genera) across all three major lineages (Supporting Information, Table S1) through fieldwork (*Bothrops atrox, Azemiops kharini*), donations from captive breeders (*Bothriechis schlegelii, Trimeresurus trigonocephalus, Vipera berus*), or from the licensed commercial trade (other species). Sample size for all species was one, except for *B. arietans,* for which two animals were sacrificed (one for molecular biology, ocular media transmission and histology and one for MSP). Laboratory animal procedures were approved by the Institutional Animal Care and Use Committee (IACUC) of the Florida Institute of Technology, and research conducted under a venomous reptiles permit issued by the State of Florida. Snakes were housed individually in 1750 cm^2 ventilated plastic enclosures on a 12:12 h dark:light cycle, with water available *ad libitum*. Laboratory mice were offered as food at least twice per month. Snakes were placed individually in a small animal induction chamber and observed while exposed to inhalant anaesthetic (halothane). When snakes exhibited no righting reflex, they were removed from induction chamber and euthanized by decapitation. In the field, snakes were anaesthetized with an intracoelomic injection of lidocaine and euthanized by decapitation.

Eyes were extracted from freshly euthanized snakes and stored in RNAlater (Ambion) at -80°C. Total RNA was extracted using a combination of TRIzol® and the PureLink™ RNA Mini Kit (Life Technologies/Ambion) following the manufacturer's protocol. Between 100 ng and 500ng of total RNA was primed with 1 µl of oligo(dT)20 (50 µM, Invitrogen). First strand complementary DNA (cDNA) was synthesized using Superscript III™ reverse transcriptase (Invitrogen) according to the manufacturer's instructions. RNA complementary to the cDNA was removed by 2 units of *E. coli* RNase H (Ambion) and incubated at 37°C for 20 minutes. Visual opsin genes were amplified by PCR and cloned using protocols reported by (Simões *et al.*, 2015; 2016b). Eight positive clones of each amplicon were sequenced in both directions.

Viper specimens were dissected extensively for a range of tissues such that in most cases there is no associated museum voucher specimen. As an alternative, we provide DNA barcode 'vouchers' (Supporting Information, Table S1). Genomic DNA was extracted from the Trizol RNA extraction DNA phase following the manufacturer's protocol, and 16s rRNA sequence data were generated using protocols reported by Simões *et al.* (2015; 2016b).

Alignment and phylogenetic analysis

DNA sequences were aligned with published sequences from other squamates including other snakes, including vipers (Supporting Information, Table S1) with MAFFT v.7.388 (Katoh *et al.*, 2002) (settings as follows: algorithm: auto; gap penalty: 3; off-set value: 0.1) implemented in Geneious R8 and manually inspected. Three alignments were created for each for the three visual opsin genes identified (*sws1*, *lws*, *rh1*). jModelTest 2 (Darriba *et al.*, 2012) was used to ascertain that GTR+G+I was the best-fit model of sequence evolution for all three opsin genes according to AIC and BIC scores. Phylogenetic analyses were conducted using Maximum Likelihood (ML) and Bayesian Inference (BI) approaches. ML analyses were

run with RAxML v8 (Stamatakis, 2014) using majority rule bootstopping criteria (Pattengale *et al.*, 2010); randomized MP starting trees, and a fast hill-climbing algorithm. BI analyses were run with Mr. Bayes v3.2 (Ronquist *et al.*, 2012) for 1,000,000 generations with chains sampled every 100 generations (after 25% of trees were discarded as burn-in), random starting trees, 4 chains (3 hot and 1 cold), and convergence was assumed when the standard deviation of split frequencies fell to below 0.01. Gekkotan lizard sequences (Supporting Information, Table S1) were used to root *sws1* and *lws* trees, and non-snake squamates to root *rh1* trees.

SELECTION PRESSURE ANALYSIS AND ANCESTRAL STATE RECONSTRUCTION

Several studies have shown the power of the ratio of non-synonymous to synonymous substitutions per site to identify adaptive evolution in systems ranging from genomes (Amemiya *et al.*, 2013; Castoe *et al.*, 2013) to genes responsible for sensory capabilities (Zhao *et al.*, 2009b; Weadick & Chang, 2012; Yoder *et al.*, 2014). Although clade- and branch-site models to test for positive selection across specific lineages are widely used, codon-based models have been criticized for failing to detect functionally important sites in visual opsin genes that have been determined through *in vitro* expression (Yokoyama *et al.*, 2008). However, recent studies have shown a strong correlation between amino acid sites under positive selection and sites with functional importance (Loughran *et al.*, 2012), including in visual pigments (Schott *et al.*, 2014; Simões *et al.*, 2016b). Therefore, we used selection test analyses here to identify evolutionary patterns in visual opsin genes.

Codeml from the PAML 4.7 package (Yang, 2007) was used to estimate non-synonymous (dN) and synonymous (dS) substitution rates and their respective ratio (dN/dS or ω) for the *sws1, lws* and *rh1* genes in vipers (without outgroups) using a phylogenetic tree congruent

with that of Pyron et al. (2013; though following that of Wüster *et al.*, 2008 for the relationships among *Echis, Causus* and *Cerastes*) and a sequence alignment in which indels were removed if present in only one taxon or recoded as missing data if present in more. Splice variants were removed from the analysis. We sought evidence of purifying, positive or neutral selection across phylogenetic branches, amino-acid sites (codons), and both branches and sites using Branch (Yang *et al.*, 2000), Site (Yang, Wong, & Nielsen, 2005), Branch-Site (Zhang *et al.*, 2005) and Clade (CmC: Bielawski & Yang, 2004; Weadick & Chang, 2011) models. Models were compared using the Likelihood Ratio Test (LRT) and simpler models were rejected where $P<0.05$. We tested the hypotheses that signatures of selection are not significantly different between pit vipers and non-pit vipers, and between pit vipers and all other snakes (including non-pit vipers), the latter by adding our new viper data to the visual opsin gene dataset analysed by Simões et al. (2016b).

Ancestral visual opsin gene sequences were estimated by marginal and joint reconstruction using Codeml. Ancestral states were reconstructed for vipers without outgroups.

SPECTRAL TRANSMITTANCE OF OCULAR MEDIA

For two pit vipers (*Agkistrodon contortrix*, *Crotalus durissus*) and one non-pit viper (*Echis coloratus*) the lens and brille (= 'spectacle', the specialized scale covering the eye) were dissected and stored dry at -20°C. Immediately after thawing they were mounted in purpose-built holders in air in front of an integrating sphere within a Shimadzu 2101 UVPC spectrophotometer. Transmission at 700 nm was set to 100% and tissue scanned at 1 nm intervals from 300–700 nm. A single lens and both brilles were scanned for *C. durissus* and *E. coloratus*, whereas in *A. contortrix* both lenses and both brilles were scanned.

Lenses were small (axial diameters for *E. durissus*, *C. coloratus* and *A. contortrix*: 1.35, 1.80 and 1.80 mm, respectively) limiting the amount of light transmitted, and the use of an integrating sphere reduced sensitivity further, thus the raw data are noisy at short wavelengths where lamp output is low. Data from scans were therefore smoothed using a cubic Savitzky-Golay filter (data frame length 51 nm) using Matlab R2011a (The MathWorks Inc, MA, USA).

HISTOLOGY

We sectioned one retina each of *Bitis arietans, Cerastes cerastes, Echis coloratus* and *Vipera berus*. Primary fixation was of whole heads (eyes punctured) in a solution of 2.5% glutaraldehyde and 2% paraformaldehyde in 0.1M pH 7.4 cacodylate buffer for 3h. Secondary fixation in 1% osmium tetroxide in 0.1M cacodylate buffer for 1.5h at room temperature took place after three 1h rinses in 0.1 cacodylate buffer. After three 20 minute cacodylate buffer rinses eyes were removed (orientation not recorded) and dehydrated in a progression of ethanol dilutions: 30%, 40% and 50% for 15 minutes each; 70% overnight; 80%, 90%, 95% and 100% (x3) for 15 minutes each. Samples were embedded in a 1:1 mixture of ethanol:resin on a rotary mixer for 12h and then 100% resin for 10h, before changing to fresh resin that was polymerized at 70°C for 36h. Transverse and tangential sections (1-2µm) of the central retina were stained with toluidine blue for light microscopy; micrographs were taken on a digital Zeiss microscope. For electron microscopy we used the same blocks to produce ultrathin sections of the outer retina. These were “stained” with uranyl acetate and lead citrate and viewed in a LEO 912 microscope.

IMMUNOHISTOCHEMISTRY

For one pit viper (*Crotalus durissus*) and one non-pit viper (*Echis coloratus*), a whole head was fixed by immersion in 4% (w/v) paraformaldehyde in 0.01 M phosphate buffered saline (PBS, pH 7.4) for approximately 3 hours with the brille removed and the eye punctured in situ to facilitate fixative penetration. After fixation the eyes were removed, washed three times in PBS, and stored in PBS with 0.05% sodium azide at 4°C. Orientation of the eyes was not recorded.

Opsin immunohistochemistry was performed on frozen transverse sections of the retina (i.e., sectioned perpendicular to the retinal layers). The retina was isolated from the eyecup, cryoprotected by successive immersion in 10%, 20% and 30% (w/v) sucrose in 0.1 M phosphate buffer (PB, pH 7.4), and transferred to Tissue Freezing Medium (Leica Biosystems, Wetzlar, Germany). The retina was embedded and frozen in a block of Tissue Freezing Medium with appropriate orientation, sectioned at a thickness of 16 µm with a cryostat, and collected on SuperFrost slides (Menzel GmbH, Braunschweig, Germany).

Immunolabelling followed standard protocols. Briefly, the sections on the slide were preincubated for 1 h in PB with 0.5% Triton X-100 and 10% normal donkey serum (NDS). Incubation was overnight at room temperature in the primary antibody/antiserum solution, made up in PB with 3% NDS and 0.5% Triton X-100. Rod opsin RH1 was detected with the mouse monoclonal antibody rho4D2 (dilution 1:500). Cone opsins were detected by the rabbit antiserum JH492 (dilution 1:2000) against the longwave-sensitive (LWS) cone opsin, and by the goat antiserum sc-14363 (dilution 1:500) or by the rabbit antiserum JH455 (dilution 1:5000) against the shortwave-sensitive (SWS1) cone opsin. Double immunofluorescence labelling for the simultaneous visualization of LWS and SWS1 opsin was achieved by incubation in a mixture of the two antisera JH492 and sc-14363. Rho4D2 was kindly provided by R. S. Molday (Hicks & Molday, 1986), JH492 and JH455 were kindly

provided by J. Nathans (Wang *et al.*, 1992) , and sc-14363 was purchased from Santa Cruz Biotechnology Inc., Heidelberg, Germany. These antibodies have been used in several previous studies to reliably label the respective opsins in a range of mammals (e.g., Schiviz *et al.*, 2008; Glosmann *et al.*, 2008; Schleich *et al.*, 2010; Moritz *et al.*, 2013). JH492 and JH455 also have labelled the LWS and SWS1 opsins, respectively, in dipsadine snakes (Hauzman *et al.*, 2014) , and sc-14363 has labelled the SWS1 opsin in birds (Nießner *et al.*, 2011). Binding sites of the primary antibodies were visualized by indirect immunofluorescence, with a 1 h incubation of the sections in the secondary antiserum. We used Alexa 647-conjugated donkey anti-mouse IgG for the rod opsin labelling, and Alexa 488-conjugated donkey anti-goat IgG and Alexa 647-conjugated donkey anti-rabbit IgG, respectively, for the cone opsin labelling. JH492 and sc-14363 double-labelling was visualized by incubation in a mixture of Alexa 488-conjugated donkey anti-goat IgG and Cy5-conjugated donkey anti-rabbit IgG. Omission of the primary antibodies from the incubation solution resulted in no staining.

For some sections, Alexa 594-conjugated peanut agglutinin (PNA; dilution 1:100; Molecular Probes, Eugene, OR, USA) was used in conjunction with either JH492 or sc-14263. PNA is a general cone marker in mammals, chicken and goldfish (Blanks & Johnson, 1984), and we were interested to see which photoreceptor types it would label in vipers. PNA was mixed with the secondary antiserum for a 1 h incubation. For some sections, the secondary antiserum solution also contained 4,6-diamidino-2-phenylindole (DAPI) as a fluorescent nuclear stain to reveal the general retinal layering. All sections were coverslipped with an aqueous mounting medium (AquaPoly/Mount, Polysciences Inc., Warrington, PA, USA).

For further assessment of the cones, one half-retina each of *Crotalus durissus* and *Echis coloratus* was immunolabelled for the cone opsins free-floating, then flat-mounted on slides with the photoreceptor side up. Here incubation time in the mixture of the two opsin

antisera JH492 and sc-14363 was extended to three days at room temperature, incubation in the secondary antiserum mixture was for 1 h.

Stained sections were analyzed with a Zeiss Axioplan 2 microscope equipped with epifluorescence. Micrographs were taken with a CCD camera and the Axiovision LE software (Carl Zeiss Vision, Germany). The immunolabelled flat mounts were analyzed with a laser scanning microscope (LSM) Olympus FluoView 1000 using the FV 1.7 software (Olympus). LSM images and z-stack projections were examined with ImageJ (http://imagej.nih.gov/ij/); cells were counted using the cell counter plugin. Images for illustration were adjusted for brightness and contrast using Adobe Photoshop. For convenience and the benefit of red-green-blind readers, SWS1 label was rendered in magenta, and LWS label in green, irrespective of the fluorescent dye used to visualize the label.

PHOTORECEPTOR DENSITY ESTIMATES

Limited estimates of photoreceptor densities were obtained from the flat-mounted half-retinas. Visualizing the photoreceptor inner and outer segments with differential interference contrast (DIC) optics allowed their counting in favourable patches across the retinas. In the *E. coloratus* retina used for immunolabelling, outer LWS cones were largely damaged or lost. Here we resorted to a semithin tangential section from another eye that grazed the array of outer cones, directly showing their areal packing.

MICROSPECTROPHOTOMETRY (MSP)

MSP protocols were similar to those described by (Loew, 1994; Fleishman *et al.*, 2011). Eyes from three vipers, the viperine *Bitis arietans* and crotalines *Agkistrodon contortrix* and *Crotalus atrox* (Supporting Information, Table S1), were prepared under infrared or dim red-

light illumination. The *B. arietans* and *A. contortrix* specimens were not the same individual animals for which visual opsins were sequenced. The vipers were dark-adapted for at least 12 hours before being euthanized. Eyes were enucleated under dim red light, and placed in cold PBS and shipped on ice to Cornell University. Upon arrival, the eyes were washed and trimmed in fresh PBS and hemisected around *ora serrata*. The resulting eyecups were placed in fresh PBS (pH 7.2) made hyperosmotic with 6% sucrose and the retina was teased away from the RPE. Small pieces of retina were transferred to coverslips where they were chopped with scalpel blades before being sandwiched with another cover slip.

RESULTS

OPSIN GENE COMPLEMENTS AND PHYLOGENETIC ANALYSIS

Three opsin genes were amplified in all vipers: *sws1*, *lws* and *rh1*, their identity confirmed by BLAST searches and by phylogenetic analysis (data not shown). Our sequence alignments for the expressed opsin genes included between 95% and 98% of the coding region. Alternative splicing sites were found at the exon 1/exon2 boundary in two and one of the eight clones sequenced of the *sws1* of each of *Bothrops atrox* and *Agkistrodon contortrix,* respectively, resulting in the extension of 39 nucleotides (13 amino-acids) in the former and removal of exon 2 in the latter.

For each opsin alignment ML and BI analyses estimated similar tree topologies (Supporting Information, Figs. S1–S3). Inferred gene trees for *rh1* and *sws1* are generally concordant with published species molecular phylogenies (Wüster *et al.*, 2008; Pyron *et al.*, 2013), but the *lws* tree lacks a monophyletic Crotalinae. Differences between the lws and

the *sws1* and *rh1* gene trees are, however, associated with internal branches that are not well supported by ML bootstrap or Bayesian posterior probabilities.

MICROSPECTROPHOTOMETRY

We made 120 MSP readings, at least 30 per species, and found three pigments in each sampled viper (Fig. 1). As far as could be determined, the probable RH1 pigment (λ_{max} ca. 495–500 nm) appears to be confined to rods, which contain this pigment only. The putative SWS1 pigment (λ_{max} ca. 350–420 nm) occurs in smaller cones and LWS (λ_{max} ca. 540–555 nm) in larger cones. Double cones could not be distinguished from single cones within macerated retinas.

Our measured λ_{max} values are similar to those predicted (from opsin amino acid sequences) for the two analysed species for which gene sequence data were generated (the viperine *Bitis arietans* and the crotaline *Agkistrodon contortrix*), except for the *A. contortrix* SWS1 which had an λ_{max} value predicted to be in the UV but measured at 416 nm (see Supporting Information, Tables S2–S4). The other crotaline subjected to MSP, *Crotalus atrox,* has a presumed RH1 pigment with a λ_{max} value (497 nm) close to that predicted for its congener *C. durissus* (500–505 nm), while the λ_{max} values for the *C. atrox* putative SWS1 and LWS are notably different from those predicted for *C. durissus* (374 and 541 nm versus UVS and 555 nm, respectively).

SPECTRAL TUNING PREDICTIONS AND ANCESTRAL STATE RECONSTRUCTION

Examination of the 11 critical sites (Supporting Information, Table S2) that are known to most influence spectral tuning (λ_{max}) of SWS1 visual pigment in vertebrates (Yokoyama *et al.*, 2006) revealed a highly unusual substitution at site 93 with alanine (A) replacing threonine

(T) in all Viperinae, *Azemiops kharini* and *Bothrops atrox* (all amino acid positions reported here correspond to bovine rhodopsin). Threonine is present at SWS1 site 93 in all other pit vipers (Supporting Information, Table S2) and is reported in most other studied reptiles, birds and mammals (Hunt *et al.*, 2007; Carvalho *et al.*, 2011; Odeen & Hastad, 2013; Simões *et al.*, 2015). This T93A substitution in vipers is unreported elsewhere among vertebrates. A substitution at SWS1 site 118 from serine (S) to threonine was found in the viperines *Echis coloratus*, *Vipera berus* and *Cerastes cerastes*, the azemiopine *A. kharini* and crotaline *B. atrox* (Supporting Information, Table S2). This S118T also occurs in the SWS1 opsin of some other colubroid snakes (Simões *et al.*, 2015) and is predicted to increase the λ_{max} by 3 nm (Yokoyama *et al.*, 2006).

The only RH1 spectral site varying among vipers is site 83 (Supporting Information, Table S3), with aspartic acid (D) occurring in the viperines *E. coloratus*, *B. arietans*, and *C. cerastes,* and the crotalines *C. durissus* and *B. atrox,* in contrast to asparagine (N) occurring in all other sampled vipers (and the majority of squamate reptiles (Simões *et al.*, 2015; Simões *et al.*, 2016b). A change at site 83 from D to N is predicted to reduce the λ_{max} of RH1 by 6 nm from 500–501 nm (Nathans, 1990). The LWS amino-acid sequence lacks any variation in five known spectral sites among the sampled vipers (Supporting Information, Table S4), which have an AHYTA amino acid pattern at sites 180-197-277-285-308, such that they are predicted to have an LWS pigment with λ_{max} of ca. 555 nm (Asenjo *et al.*, 1994).

Applying predictions of λ_{max} to the estimated ancestral opsin gene sequences (see (Simões *et al.*, 2016b) for comments on tuning predictions in snakes) suggests that a ca. 555 nm λ_{max} LWS opsin was present in the ancestral viper and retained throughout viperid evolution (Fig. 2; Supporting Information, Table S4). The ancestral viper is reconstructed as having a 500–501 nm λ_{max} RH1 with a decrease to 491–496 nm (following a D83N

substitution) in the ancestor of Azemiopinae+Crotalinae (and independently in the viperine *Bitis arietans*) (Fig. 2; Supporting Information, Table S3). The ancestral viper SWS1 is reconstructed as having 93A, with an A93T change in the ancestral crotaline, but with the ancestors of all major lineages retaining a UVS λ_{max} (ca. 360 nm), increasing by ca. 3 nm four times independently within vipers (Fig. 2; Supporting Information, Table S2). The S118 in the SWS1 opsin is reconstructed as likely to have been present in the ancestral viper, with an S118T change occurring independently four times, in the ancestor of *Echis*+*Cerastes*, in *Vipera berus*, in *Azemiops kharini* and in *Bothriechis schlegelii.*

SELECTION ESTIMATES

Although models that include positive selection have a better fit than models without, ω estimates are all substantially less than 1 for viperids, suggesting that all three visual opsin genes are generally under purifying selection (Supporting Information, Table S11). Compared to snakes as a whole (compare Tables S6 and S11), viperid *sws1* has a lower ω (0.07679 versus 0.107), viperid *rh1* a much higher ω (0.6476 versus 0.237), and viperid *lws* a slightly higher ω (0.3658 versus 0.312). Viperid *rh1* and *lws* have ω estimates higher (and viperid *sws1* lower) than average for vertebrate coding genes (0.12; Fay & Wu, 2003). The viperid data thus match the snake-wide pattern found by Simões et al. (2015, 2016b; see also Supporting Information, Table S6) of greater overall purifying selection in *rh1* and *lws* than in *sws1,* in contrast to the pattern found in, for example, mammals (Zhao *et al.*, 2009a; Invergo *et al.*, 2013).

Although CmC analysis found evidence for significant differences in selection patterns between pit vipers and other snakes (Supporting Information, Table S9), we note that significance is marginal (p = 0.04) for *rh1*, that there are no significant differences

between pit and non-pit vipers for all three visual opsin genes when CmC is applied only to the viperid data (Supporting Information, Table S14), and that gene-wide selection estimates do not differ substantially between pit vipers and other snakes (Supporting Information, Table S5) and particularly between pit vipers and non-pit vipers (Supporting Information, Table S10). Thus, we conclude that there is no compelling evidence for significant changes in opsin gene molecular evolution associated with the acquisition of IR-detecting pit organs in vipers.

For viperids, Bayesian Empirical Bayes (BEB) estimated by site models (Supporting Information, Table S12) detected positive selection at spectral sites T93A and S118T in *sws1*, D83N in *rh1,* and 180 in *lws*. Evidence of positive selection in viperids was also found in amino acid sites involved in stabilization of the retinal pocket: site 133 in *lws* and sites 123 and 223 in *rh1*. More complex site models (M8 β&ω and M2a) are a significantly better fit than simpler models (M7β and M1a) in all cases. Under branch-site models (Supporting Information, Table S13) where Viperinae, Crotalinae and Azemiopinae were marked alternatively as the foreground lineage, spectral site T93A in *sws1* is identified as being under positive selection in pit vipers (Crotalinae), indicating that the latter group is primarily responsible for the detection of positive selection at this site for viperids as a whole using site models M2a and M8 β&ω (see above). Many of the sites identified as being under positive selection in viperids are similarly found to be under positive selection across snakes as a whole (Table S7).

LENS AND BRILLE SPECTRAL TRANSMITTANCE

Spectral transmittance characteristics of ocular structures are very similar in the three species examined (Fig. 1). The extracted lenses of *Echis coloratus*, *Crotalus durissus* and

Agkistrodon contortrix were spherical and clear, and all had high UV transmission with wavelengths of 50% transmittance between approximately 301 and 318 nm. The brilles were also macroscopically transparent, with 50% transmittance at approximately 311 nm, 309 nm and 315 nm in *E. coloratus*, *C. durissus* and *A. contortrix*, respectively. Although not subjected to analysis, all other viper eyes dissected for this study had superficially transparent lenses and brilles.

RETINAL HISTOLOGY

The central region of the retina of the viperines *Bitis arietans, Cerastes cerastes, Echis coloratus* and *Vipera berus* was studied in transverse and tangential semithin sections. In *C. cerastes* and *V. berus* embedding material was only partially polymerized, resulting in imperfect sections and compromised histological quality. Light microscopic investigation showed that all four species have a two-tier arrangement of photoreceptors (for images of *B. arietans* and *E. coloratus* see Figs. 3 and 4, respectively), with long single cones with bulky inner segments lying scleral to rods (outer tier), and short, slender single cones in the inner tier. In *B. arietans,* rods and cones are approximately equal in number. In *B. arietans*, there are approximately four times as many short single as long single cones; whereas in *E. coloratus* their ratio is approximately equal. In *C. cerastes* the outer retina is similar to that of *B. arietans* whereas in *V. berus* a clear identification of rods and small single cones was not possible because of technical problems with sectioning. In *C. cerastes* there are an approximately equal number of nuclei in the outer and inner nuclear layers, in *B. arietans* the inner layer nuclei outnumber those of the outer layer by approximately 1.6:1, whereas in *C. durissus* and *E. coloratus* the outer:inner layer nuclei ratio is approximately 1.3:1 and 1.0–1.3:1, respectively. Interestingly, all photoreceptor nuclei were evenly stained, suggesting

that snake rod nuclei do not stain darker than cone nuclei (unlike the situation in e.g., actinopterygian fishes (H.-J. W., pers. obs.) and mammals (Solovei *et al.*, 2009).

Ultrastructural observations revealed no unusual features. Rod and cone inner segments were packed with small mitochondria, and in the outer plexiform layer the general arrangement of small rod spherules with one or two synaptic ribbons in a position distal to the much larger cone pedicles with more numerous ribbon-associated synaptic complexes was confirmed.

RETINAL IMMUNOHISTOCHEMISTRY

For *Echis coloratus* and *Crotalus durissus*, suitable tissue was available for opsin immunolabelling in transverse retinal sections and unsectioned flat mounts. The retinas of both the viperine *E. coloratus* and the crotaline *C. durissus* are rod dominated (Fig. 5). The rho4D2 antibody labelled RH1 strongly in rod outer segments; with over-exposure it was possible to detect fainter labelling of rod somata and even rod axon endings in the outer plexiform layer (Fig. 5). Rod somata are arranged across the thickness of the outer nuclear layer, revealing the extent of this layer. In contrast to *E. coloratus*, in *C. durissus* only a few rods were labelled through to their axon endings.

A striking feature of the *E. coloratus* retina is its two-tiered arrangement of cone photoreceptors (Fig. 6). The more scleral (outer) tier comprises only the stout outer segments and ellipsoids of large single cones. The somata of these outer cones reside in the ONL like those of all other photoreceptors, they are connected to the inner segments by stalks traversing the inner tier of photoreceptors. The inner tier comprises (in addition to the myoids of large single cones) the inner and outer segments of rods, small single cones and double cones. The large and small single cones stain exclusively for LWS (antiserum JH492)

and SWS1 (antiserum sc14363), respectively. SWS1-labelled inner tier cones are less numerous than LWS-labelled inner tier cones (Fig. 8; see below). Double cones all appear morphologically unequal, comprising a principal cone with thick inner segment and an accessory cone with slender inner segment. Both members of double cones are labelled for the same visual pigment, variably LWS or SWS1 (Figs. 6, 9). The proportion of LWS double cones among the LWS cones is approximately or less than 10% (c.f. Fig. 8), the SWS1 double cones are much less common. Double-labelling for cone opsins and PNA show that PNA labels all LWS cones and no SWS1 cones (Figs. 6, 9).

Crotalus durissus has a higher cone density than *E. coloratus*, with a dominance of LWS cones over SWS1 cones (Figs. 7, 8). Nowhere were two tiers observed but, surprisingly given previous work on vipers, both larger (LWS-labelled) and smaller (SWS1-labelled) single cones are present (Fig. 7). LWS-labelled double cones are present at low density, and we observed a few possible SWS1 double cones (Fig. 9; see Discussion). Both members of double cones contain the same visual pigment. As in *E. coloratus,* in *C. durissus* PNA labels all LWS cones and no SWS1 cones (Figs. 7, 9). Cone outer segments are considerably larger in *E. coloratus* than in C. *durissus* (Figs. 8, 9).

In both *E. coloratus* and *C. durissus*, cone inner segments are thicker than those of rods, and there is no indication of co-localization of SWS1 and LWS in any single photoreceptor outer segment. There is also no indication of RH1 co-localization with either SWS1 or LWS, but the generally high density of rods makes this more difficult to ascertain with confidence. Antiserum JH455, expected to label SWS1, non-selectively stained many photoreceptors in both species, seemingly more cells than all cone types combined, i.e., also at least some rods (not illustrated). Additionally, JH455 stained not only outer segments but also produced a punctate labelling in somata of the outer and inner nuclear and ganglion cell

layers. Hence the JH455 labelling differs from that in dipsadine colubrid snakes, where it is restricted to SWS1 cones (Hauzman *et al.*, 2014); the reasons for this are unknown.

PHOTORECEPTOR DENSITY ESTIMATES

Limited estimates of photoreceptor densities and proportions in *E. coloratus* and *C. durissus* were obtained from the flat-mounted half-retinas and transverse sections. Because the eyes were not oriented, no detailed topographic information about density changes across the retina or local retinal specializations is available. We could differentiate only between central retina (i.e. close to the optic nerve head) and peripheral retina. In *C. durissus*, visualization of the photoreceptor layer by DIC microscopy in the flat mount reveals the larger profiles of cone inner segments and the smaller profiles of rod inner and outer segments (Fig. 10a). In 12 sampling fields across the retina, cone density is 9,200–20,200 mm^{-2} (mean 15,400 ± 3,500 S.D.). The densities of LWS and SWS1 cones were assessed in four immunolabelled fields from central and peripheral retina (c.f. Fig. 8). The range is 11,700–19,300 LWS cones mm^{-2} (mean 16,600 ± 3,400 S.D.) and 1,800–2,500 SWS1 cones mm^{-2} (mean 2,200 ± 300 S.D.), resulting in a total of 13,900–20,500 cones mm^{-2} (mean 18,100 ± 3,000 S.D.). Thus, SWS1 cones comprise 10–15% of the cones (mean 12%). These cone densities also show marked local variations but no obvious centro-peripheral gradient. There is good correspondence between the cone densities obtained in the DIC images and the immunofluorescence images but, due to the low proportion of SWS1 cones, we cannot determine whether the cone profiles seen by DIC (Fig. 10a) represent only the LWS cone inner segments or also include the somewhat smaller SWS1 cone inner segments (c.f. Fig. 7). *Crotalus durissus* rod densities were visible in favourable small patches (see Fig. 10a) and could be assessed in eight sampling fields across the retina. Their range is 120,000–211,000

mm^{-2} (mean 166,000 ± 31,000 S.D.), showing marked local variations but no obvious centro-peripheral gradient. Adding the rod and cone densities at the various locations results in total photoreceptor densities of 134,000–225,000 mm^{-2} (mean 178,000 ± 32,000 S.D.). Cones locally constitute between 4.5% and 11.5% of the photoreceptors; comparing the DIC-derived mean rod and cone densities yields ca. 9% cones (rod:cone ratio ca. 11:1).

In *E. coloratus*, DIC visualization of the photoreceptor layer in the flat mount reveals a rather homogeneous population of smaller profiles that presumably comprise rods and small single cones, and few interspersed larger profiles of presumed large single cones (Fig. 10b). In 25 sampling fields across the retina, photoreceptor density is 116,000–178,000 mm^{-2} (mean 146,000 ± 17,000 S.D.). There is a trend for higher densities in central than in peripheral retina (mean 162,000 ± 19,000 S.D. versus 134,000 ± 9,000 S.D.), but with marked local density variations. The assessment of *E. coloratus* cone densities is less reliable. Estimates obtained in the opsin-immunolabelled sections yield an average of 4,800 inner cones mm^{-2}, comprising equal densities of inner LWS cones and inner SWS1 cones. In the opsin-immunolabelled flat-mounted half-retina (Fig. 8), inner LWS cones are more numerous than inner SWS1 cones, with the latter comprising only ca. 22% of the cones, and inner cone density is only ca. 1,000 mm^{-2}. It is possible that a large proportion of cone outer segments was lost in the flat-mounted retina, or that it represents a region of markedly lower cone density. The outer LWS cones were mostly lost in the immunolabelled retina (sections and flat mount), so their density had to be assessed in a semithin tangential section from another retina that directly showed their areal packing. In this field, their density is 12,950 mm^{-2}. Assuming ca. 20% areal shrinkage of the plastic-embedded tissue (following, e.g. (Steinberg, Reid, & Lacy, 1973)), the shrinkage-corrected density of outer LWS cones is ca. 10,000 mm^{-2}. Thus, *E. coloratus* maximally has 10,000 outer LWS cones mm^{-2}, 2,400 inner

LWS cones mm^{-2} and 2,400 SWS1 cones mm^{-2}, i.e. the SWS1 cones constitute ca. 50% of the inner cones and 16% of all cones, and the cones constitute ca. 10% of the photoreceptors. If the lower densities of inner cones seen in the flat mount are used, there would be 10,000 outer LWS cones mm^{-2}, 760 inner LWS cones mm^{-2} and 220 SWS1 cones mm^{-2}, i.e. the SWS1 cones would constitute ca. 22% of the inner cones and 2% of all cones, and the cones would constitute ca. 7.5% of the photoreceptors. Surprisingly, both the rod and the cone density are higher in *C. durissus* than in *E. coloratus* even though the latter has two tiers of photoreceptors.

DISCUSSION

We have made novel observations and discovered interesting patterns in viperid snake retinal anatomy, visual pigment spectroscopy and visual opsin gene evolution. However, our comparative, integrative examination found no evidence for the evolution of IR sensitivity having had a substantial impact on the vision of vipers in terms of ocular media transmittance, visual pigment complement or spectral sensitivity, or visual opsin gene molecular evolution.

PHOTORECEPTOR COMPLEMENTS

Although sampling was sparse, previous surveys of the anatomy of viper retinas reported a fundamental dichotomy between pit vipers and non-pit vipers. Only the latter were believed to have small single cones in addition to large single and double cones and rods (Walls, 1942; Underwood, 1967; Underwood 1970; Hirosawa, 1978; Underwood, 1997). We are aware of

only one previous challenge to this pattern, a brief report of the absence of double cones in *Cerastes cerastes* (Khattab *et al.*, 2004). We also failed to observe double cones in the (central part of the) retina of *C. cerastes* using conventional light microscopy, but neither did we observe them in *Bitis arietans* in which they are known to be present (Walls, 1942; Underwood, 1967; Underwood 1970). In contrast, we clearly identified double cones in *E. coloratus* and *C. durissus* retinas immunolabelled for the cone opsins. Double cones are rare in viper retinas and could be missed in incomplete retinal surveys. Double cones are present in most caenophidian ('higher') snakes (Underwood, 1970) and we suggest that their reported absence in *C. cerastes* requires verification.

Our immunohistochemistry provides the first evidence that, in addition to *lws*-expressing double cones at least some vipers additionally have a rare class of double cones that express only *sws1*. Two pigment-based classes of double cones is contrary to the condition reported (based on MSP data) in the natricids/ines *Thamnophis sirtalis* (Sillman *et al.*, 1997) and *T. proximus* (Schott *et al.*, 2016) and the marine elapids *Hydrophis* (*Lapemis*) *curtus* and *Hydrophis* (*Acalyptophis*) *peronii* (Hart *et al.*, 2012), although it can be difficult to identify double cones in macerated retinas during MSP. Hauzman et al. (Hauzman *et al.*, 2014) also found (by immunolabelling) no evidence for double cones of the dipsadine *Philodryas* spp. containing any visual opsin other than LWS. As far as we are aware, double cones in which both members express only *sws1* have not been reported elsewhere among vertebrates. Given that double cones in which both members express the same visual opsin are thought to be involved in achromatic aspects of vision (e.g. Pignatelli *et al.*, 2010 and references cited therein), viperids might have two (LWS- and SWS1-based) brightness-only channels, and/or some unusually complex form of colour vision. As illustrated in Figure 9, the evidence for SWS1 double cones is more convincing in the non-pit viper *E. coloratus* than

in the pit viper *C. durissus*, so further analysis will be needed before it can definitively be concluded whether there is a difference in this feature between the two groups. The reason for PNA labelling of all LWS and no SWS1 cones is unclear, PNA being a general cone marker (at least in various mammals, chicken and goldfish; (Blanks & Johnson, 1984)) that attaches to cone-specific components of the interphotoreceptor matrix. PNA labelling of cones has previously been used in colubrid snakes, but that study did not assess whether PNA labelled all cones or only LWS cones (Hauzman *et al*., 2017).

Our discovery of two size classes of single cones in the crotaline *Crotalus durissus* is at odds with the previous interpretation (e.g., Walls, 1942; Underwood, 1967; Underwood, 1970) that pit vipers have only one size class of single cone. Although we know of no previous microscopic examinations of photoreceptor anatomy in *C. durissus,* this unexpected result might also be interpreted as casting doubt on the veracity of some conclusions about photoreceptor complement in snakes based on conventional histology. In another, similar case, Sillman et al. (Sillman *et al.*, 1999; Sillman *et al.*, 2001) reported two size classes of single cones in boas and pythons *contra*, for example, Walls (1942: plate 1) and Underwood (1967; 1970). Although we do not doubt Walls' and Underwood's conclusions that photoreceptor complements in snakes are remarkably variable, we suggest that caution needs to be exercised in accepting the precision of the reported complements in each case. As with many aspects of snake vision, further research on retinal anatomy (one of the few aspects that seemed to be better known) is warranted. In conclusion, it is not the case that all pit vipers lack the small single cones present in non-pit vipers, so this is not a fundamental difference between the two groups.

Walls (1942) mistakenly considered viperids to be non-monophyletic, with non-pit and pit vipers not being each other's closest relatives. Based on the observation that several

other caenophidian snakes have the (at least superficially) same photoreceptor complement as viperines (rods, small and large single cones, double cones), Underwood (1967: fig. 12; see also Rasmussen, 1990: fig. 4) interpreted the crotaline condition as derived from a viperine-like one by loss of the smaller single cones. Our observation of two size classes of single cones in *C. durissus* undermines both these interpretations, and demonstrates that more anatomical work and explicit character mapping on more secure phylogenies are required. Walls (1942) and Underwood (1967; 1970) considered that the rods of vipers (both crotalines and viperines, independently) were evolved from (transmuted) cones, but this was based on his mistaken understanding that vipers evolved from strongly diurnal 'colubrids' with all-cone retinas, something incompatible with modern views of extant snake phylogeny (e.g., Pyron *et al.*, 2013), in which Viperidae is monophyletic and sister to a clade comprising colubrids, elapids, homalopsids and lamprophiids.

PHOTORECEPTOR TIERING

Some observers (e.g., Walls, 1942; Underwood, 1967; Underwood 1970) have reported snake retinas in which at least some cone outer segments and ellipsoids extend scleral to the rod (and some other cone) outer segments, referring to this configuration as "two tiered". Walls (1942) and Underwood (1967, 1970: 62) considered two-tiered retinas to be a characteristic of nocturnal snakes (and vipers are generally nocturnal). Two-tiered retinas are thought to be homoplastic within snakes and there are claims they are absent in vipers (Rasmussen, 1990). However, Walls (Walls, 1942) and Underwood (1967; 1970) reported a two-tier retina in *Bitis arietans,* and Govardovski & Chkheidze (1989) documented two tiers in the central (but not marginal) parts of the retina of *Vipera berus* and *Macrovipera lebetina*. Underwood (1970) examined the retina of *V. berus* with TEM but did not report a

two-tiered arrangement (such as we found), suggesting there may be spatial and/or temporal variation within a single retina in this taxon, or intraspecific polymorphism, or that Underwood's survey of the *V. berus* retina was incomplete. We observed two tiers in four viperine species, and in no case did double cones extend into the outer tier, contrary to Walls' (1942) figure 186 for the dipsadine snake *Leptodeira annulata* (but not Walls' figure 189 for the viperine *Bitis arietans*) and Govardovski & Chkheidze (1989): fig. 1) illustration of *Macrovipera lebetina*. The outer tier we observed is also much more densely packed (at least in parts) than Walls illustrated for *L. annulata.*

Although most lower vertebrates are known to have photomechanical movements originating in the cone and/or rod myoids, Walls (1942: 150, 166) stated that this was not the case in snakes, such that scleral cones in a two-tiered snake retina lie in a "condition of 'permanent dark-adaptation'". It is not clear where Walls obtained evidence that the snake two-tiered condition was not a temporary response to ambient light levels. We note that the *Bitis arietans, Echis coloratus*, *Cerastes cerastes, Vipera berus* and *Crotalus durissus* samples examined for this study were all sacrificed after being in daylight for at least two hours, and some cones being markedly scleral to rods was seen in all except the latter. However, where it is known among vertebrates, retinomotor movement is dependent not only on light levels but also on diel cycles and it can also vary with ontogeny (Burnside, 2001). Thus, the understanding that retinomotor movement is poorly developed in reptiles and that photoreceptor tiering might be a fixed condition (where it occurs in snakes) clearly warrants reconsideration. In future studies greater attention needs to be paid to potential regional variation across the retina as well as to conditions leading up to fixation in relation to light levels and diel phase. If we accept Walls' (1942: 150, 166) understanding that snake photoreceptors do not undergo photomechanical changes, however, we currently have

evidence of the two-tiered condition occurring only in some parts of retinas of some viperines, but not yet in any crotalines.

In summary, it is possible that two-tiered retinas are present in non-pit vipers but not in pit vipers, but the (spatiotemporal) retinal and taxonomic distribution of this feature needs further investigation. It remains enigmatic why the one-tiered *C. durissus* retina has a higher photoreceptor density than the two-tiered *E. coloratus* retina. Obviously, there is no packing problem requiring a two-tiered arrangement for a higher photoreceptor density.

INNER AND OUTER NUCLEI

Underwood (1970, 1997) reported more nuclei in the inner than outer nuclear layer of the retina of viperines but not of crotalines. We were able to make only approximate estimates in the samples we examined, but found no clear difference in the ratio between the two subfamilies. Underwood (1997) related the difference in inner:outer nuclei to differences in photoreceptor circuitry. However, making inferences about the possibly oligo- or polysynaptic condition of photoreceptors is not possible without being able to distinguish bipolar from other cell types (and to distinguish among various bipolar cell types), which requires more detailed examination than was possible here. Underwood (1997) seemed to consider viperines a more diurnal group (apomorphically so) than crotalines, but we are unaware of evidence to support this. Although vipers generally (both pit and non-pit) are nocturnal, it is often difficult to classify species as strictly nocturnal or diurnal, with activity patterns influenced often by (seasonally variable) environmental temperature as well as light conditions (e.g. Phelps, 2010). Although there might be some differences in the relative proportions of inner and outer nuclei in the retinas of pit- and non-pit vipers, this has yet to

be firmly established and its correlation with retinal circuitry, visual function and ecology remains unclear.

PHOTORECEPTOR POPULATIONS

We found the (crotaline) pit viper *Crotalus durissus* to have a higher rod density, but also a higher cone density than the non-pit viperine *Echis coloratus*, hence both have a similar rod:cone ratio (about 11:1 and 9–12:1, respectively). However, the very sparse taxonomic sampling, minimal sample sizes, and lack of precise knowledge about regional variation within retinas prevent us from interpreting this as a difference between these two viper groups. Contrary to our observations, previous studies have reported relatively more rods in the retinas of pit vipers than in non-pit vipers—viperines have been reported as having rod:cone ratios of < 2:1 (*Vipera berus*: (Underwood, 1970)) and 3:1 (*Bitis, Cerastes*: Walls, 1942), and crotalines as having 7:1 (*Protobothrops flavoviridis*: Hirosawa, 1978) and 20:1 ('crotalids': Walls, 1942). In conclusion, there is no firm evidence that the two groups differ fundamentally in terms of rod-cone proportions. We are unable to explain the surprising observation of only a single tier of photoreceptor somata in the predominantly nocturnal (e.g. Phelps, 2010) *Bitis arietans.*

LENS AND BRILLE TRANSMISSION

There is no notable difference in spectral transmittance of the lens or brille between the sampled pit and non-pit vipers, all transmitting visible and near UV radiation well, in line with Walls' (Walls, 1931) report that lenses of *Bitis arietans* and *Agkistrodon contortrix* are colourless. Similarly transparent lenses were found in some diurnal but all primarily nocturnal snakes sampled by Simões et al. (Simões *et al.*, 2016b). Our results for viper brilles

match those of Van Doorn & Sivak (2015) in terms of overall high transmittance, extending into the UV. These authors found the brille of their single sampled non-pit viper species (*Bitis gabonica*) to have a higher $\lambda_{50\%}$ (331 nm) than their three sampled pit vipers (303–325 nm). Our additional sampling challenges this pattern in that the non-pit viper *Echis coloratus* that we measured has a lower brille $\lambda_{50\%}$ (311 nm) than the mean value for the pit vipers (316 nm) analysed by Van Doorn & Sivak (van Doorn & Sivak, 2015). Thus, there is no evidence of fundamentally different spectacle transmittance in pit and non-pit vipers.

VISUAL PIGMENT SPECTRAL TUNING

MSP data reinforce immunohistochemistry results in locating the ca. 500 nm λ_{max} pigment (RH1) to rods and the ca. 540–550 nm λ_{max} pigment (LWS) to larger cones. Govardovskii & Chkheidze (1989) reported rods with a λ_{max} 500 nm pigment and large single and chief double cones with a 550–560 nm λ_{max} pigment in *Vipera berus* and *Macrovipera lebetina*.

There is no clear distinction between pit and non-pit vipers in terms of opsin spectral tuning. We examined single individuals of two different species of *Crotalus* for the MSP and the gene sequencing components of the study, so cannot comment further on the *C. atrox* SWS1 and LWS λ_{max} values differing from those predicted (from amino acid sequences) for *C. durissus* and other vipers. Ancestral state reconstructions and raw amino acid data indicate that amino acid substitutions at tuning sites (known for other vertebrates) within vipers have been few and of moderate amplitude. Given that the limited MSP data do not correspond well with λ_{max} predictions in several instances in vipers (and other snakes – see below) we place much more confidence in reconstructions of ancestral sequences than in reconstructions of pigment λ_{max} based on those sequences.

Change from isoleucine (I) to threonine (T) at *sws1* site 93 is predicted to cause an SWS1 short-wavelength shift of approximately 6 nm (Yokoyama, 2000), and change from proline (P) to T in the mammalian Aye-Aye decreases λ_{max} by 35 nm (Carvalho *et al.*, 2007), but there are no clear predictions about the impact of the T93A change found in all non-pit vipers and the pit viper *Bothrops atrox*. Although the only species with an A93 for which we have MSP data (*Bitis arietans*) has an λ_{max} (357 nm) almost 60 nm less than the only species with a T93 for which we have data (*Agkistrodon contortrix*), it is unlikely that this site alone is responsible for the substantial difference because other snakes with T93 have an SWS1 λ_{max} of 360 nm (Davies *et al.*, 2009). Variation at *sws1* site 93 has no notable effect on avian spectral tuning (Wilkie *et al.*, 2000; Shi & Yokoyama, 2003; Carvalho *et al.*, 2007; van Hazel *et al.*, 2013).

The shortwave visual pigment of the only viper species with *sws1* A93 sampled for MSP (*Bitis arietans*) had an λ_{max} very close to the 360 nm predicted from the amino acids at known tuning sites. In contrast, the λ_{max} of the *B. arietans* LWS pigment (537 nm) is substantially lower than predicted from its AHYTA amino acids at sites known to be key to spectral tuning of LWS pigments in other vertebrates (Asenjo *et al.*, 1994). This suggests that sites additional to those known in other vertebrates are important in snake LWS spectral tuning. Or that other factors (also) effect tuning in these snakes.

The greatest discordance between λ_{max} values measured by MSP and predicted from amino acid sequences is for *Agkistrodon contortrix* SWS1 (416 versus 360 nm). This may be explained by possible non-conspecificity of the two different individuals used for MSP and gene sequencing (this taxon has had a contentious, unstable taxonomy: Burbrink & Guiher, 2014), and/or because λ_{max} predictions based largely on studies of non-squamate vertebrates (e.g., Yokoyama, 2008) do not always extrapolate well to snakes (see also

(Simões *et al.*, 2015; Simões *et al.*, 2016a, Simões *et al.*, 2016b). Alternatively, the species (and perhaps individuals) are polymorphic. Visual pigment and opsin polymorphism has been reported in several vertebrates (Tan & Li, 1999; Jacobs *et al.*, 2002; Veilleux & Bolnick, 2009), including snakes (Simões *et al.*, 2016b; Hauzman *et al.*, 2017) but its detection is dependent on denser intraspecific sampling than which has typically been carried out to date.

Some visual pigment λ_{max} predictions from opsin sequences have also been falsified in other snakes subjected to both MSP and gene sequencing (e.g., Sillman *et al.*, 1999; Davies *et al.*, 2009). These departures from predictions for snakes are especially notable for LWS because predictions for this pigment class seem to be particularly robust for other vertebrates. If an additional tuning site, previously unknown for vertebrate LWS, might be operating in snakes, then the most likely candidate that can be identified from current data is site 174, which is phenylanaline (F; a neutral hydrophobic amino acid) in *A. contortrix* (which conforms to predictions) but leucine (L; an aliphatic non-polar amino acid) in *B. arietans, P. regius* and *X. unicolor* (which have surprisingly low λ_{max} values). Intriguingly, *lws* site 174 is under positive selection in snakes, but other factors might also be involved in λ_{max} tuning (e.g., chromophore exchange, particularly likely in aquatic species: (Lythgoe, 1979)). Further studies using site-directed mutagenesis and *in vitro* expression are clearly required to clarify snake visual pigment tuning.

VISUAL OPSIN COMPLEMENTS

Our finding that all vipers we sampled express three visual opsin genes (*rh1, lws, sws1*) provides additional support for the hypothesis (Davies *et al.*, 2009; Simões *et al.*, 2015; Simões *et al.*, 2016a, Simões *et al.*, 2016b) that the ancestral snake possessed these three

visual opsin genes and lacked the other two (*rh2, sws2*) present in the ancestral vertebrate (e.g., (Davies, Collin, & Hunt, 2012)). The acquisition of IR sensitivity thus had no impact on visual opsin gene (or corresponding pigment) complement in vipers.

To the best of our knowledge, alternative splicing sites have not been reported in functional visual opsin genes (amplified from cDNA) in other vertebrates, including other snakes. The two instances discovered here would have been overlooked if we had not sequenced multiple clones. Although that makes it difficult to interpret negative occurrences in other taxa, we suggest that phylogeny (rather than chance alone) explains that the two known occurrences are within viperid *sws1*. Disruption of the exon 1/exon 2 boundary would seem likely to produce a non-functional pigment.

MOLECULAR EVOLUTION OF VISUAL OPSIN GENES

Although we found no compelling evidence for different signatures of selection in pit viper visual opsin genes, we identified positive selection in vipers at visual opsin amino acid sites of known functional importance, including tuning sites (*lws* site 180, *sws1* sites 93 and 118 and *rh1* site 83) and sites responsible for retinal pocket stabilisation (*lws* site 133 and *rh1* sites 123 and 223). Little is known of the effects of amino acid substitutions at sites linked with retinal binding (though we note that some were found also to be under positive selection in other, non-viperid snakes by Simões *et al.* (2015), but some additional comments can be made on the spectral tuning sites under positive selection.

Site 180 in *lws* (invariant in vipers) has been found to be under positive selection in other vertebrates, including snakes (Simões *et al.*, 2015; Simões *et al.*, 2016b), though S to A substitution here short-wavelength shifts LWS λ_{max} by only 5 nm (Asenjo *et al.*, 1994). Substitutions at *rh1* site 83 from D to N and *sws1* site 118 from S to T are known to impart a

λ_{max} shift of only 6 nm (Nathans, 1990) and 3 nm (Wilkie *et al.*, 2000), respectively, and the *sws1* T93A substitution has an unknown effect. Thus, positive selection has been detected at spectral sites not known to have substantial tuning effects, but these substitutions have occurred independently within vipers and suggest that fine-tuning of visual pigment λ_{max} is of some importance in viper sensory ecology. Further conclusions are limited by lack of extensive taxon sampling for MSP data, and obvious inadequacies in spectral tuning predictions for snakes based on amino acid sequences.

Lack of evidence for positive selection at functional sites was previously used to question methods used to identify positive selection (Yokoyama *et al.*, 2008), but subsequent studies have detected positive selection at such sites in other vertebrates (Schott *et al.*, 2014) including snakes (this study; Simões *et al.*, 2015; Simões *et al.*, 2016b). Functional studies of the uptake/release of retinal by photoreceptors, and measurements of visual pigment thermal stability, combined with site-directed mutagenesis and *in vitro* expression, may clarify how photoreception is impacted by changes at sites under positive selection in snakes but not other vertebrates.

SENSORY TRADE-OFF

We find no evidence of a trade-off in terms of diminution or other alteration of vision (at least for visual media, visual opsins, and photoreceptor complement) coincident with the acquisition of IR sensing in vipers. Despite the reported inverse relationship between eye and pit size in pit vipers (Liu *et al.*, 2016), pit vipers retain the same visual opsins as non-pit vipers and there is no compelling evidence for differences in patterns of visual opsin gene selection in the two groups. The one previously supposed major difference, the lack of small

single cones in crotalines, was found to at least not be universal within pit vipers (present in *Crotalus durissus*).

Our study finds one possible anatomical difference between pit and non-pit vipers – a two-tiered retina with some greatly elongate single large cone myoids in viperines but not crotalines. However, sampling is extremely sparse (both taxonomically and across different regions of single retinas), outgroup data are not sufficient to infer the possible direction of evolutionary changes between the one- and two-tiered state, and the functional significance of these differences are not clear. Our findings should therefore be interpreted with these caveats in mind.

Why has the acquisition of IR sensing in pit vipers had no major discernible impact on the evolution of the visual system (at least in terms of ocular media transmittance and the complement and molecular evolution of photoreceptors and visual opsin genes), given strong evidence (and plausible theoretical basis) for trade-off in other sensory systems? A possible explanation is that IR sensing in pit vipers is intimately integrated with vision operating in the 300–800 nm waveband (Bullock & Diecke, 1956; Terashima & Goris, 1975; Goris & Terashima, 1976; Hartline *et al.*, 1978; Newman & Hartline, 1981; Berson & Hartline, 1988; Goris, 2011). Electrophysiological and histological data indicate that information from the IR sensory organs is routed entirely to the optic tectum such that pit vipers construct "a broad-band image that contains the colour "infrared" in addition to the… …colours detected by the lateral eyes" (Goris, 2011). Whether IR is interpreted as a colour is, as yet, unknown and its demonstration would require appropriate psychophysical experiments, but clearly IR information is combined in the central processing of visual inputs in these snakes. Thus, the acquisition of IR detection, via apomorphic pit organs, resulted in an enhancement of the existing visual system, and the integration of novel sensory input into an established

neural vision processing centre, rather than establishing a competing sensory modality. The strength of selection against 'excess' capacity that causes sensory trade-offs depends on the energy limitations of a given system (Niven & Laughlin, 2008). Thus, an alternative or additional explanation for why there might not be a substantial trade-off between viper eyes and pit organs, though more speculative and less compelling, is that there is some currently unknown aspect of (especially viperid) snake physiology and/or their environments that presents a much less energy-limited system than in other studied cases.

Pit vipers are not the only IR sensing snakes. At least some pythons and boas also have IR detection (Goris *et al.*, 2007; Goris 2011) that evolved independently from that in vipers. Although they use similar genetic machinery to that employed in pit-viper IR sensing to at least some extent (Gracheva *et al.*, 2010), pythons and boas have seemingly less complex but more numerous, morphologically variable and variably positioned (often labial) pits that are differently neurally connected to the optic tectum (Goris, 2011). The present study is limited to pit vipers because IR sensing in vipers is much more strongly associated with the presence of a single type of anatomically complex pit, because of the previous evidence (now known to be incorrect) that pit vipers possess one fewer type of retinal photoreceptor than non-pit vipers, and because the precise taxonomic limits of IR sensing and marked variations in retinal anatomy are not known in pythons, boas and their closest relatives (pythons and boas are not each other's closest relatives and may have, at least to some extent, evolved IR sensing independently themselves). The presence of IR sensing in other snakes presents an opportunity to expand the analysis of the links between this and normal vision, and to test the generality of our findings for pit vipers.

CONCLUDING REMARKS

Although we find no evidence of a trade-off in the visual system during evolutionary acquisition of infrared pit organs in crotaline vipers, our study has highlighted a potential anatomical difference between pit vipers (two-tiered retina absent) and non-pit vipers (two-tiered retina present) but which needs more detailed investigation to confirm that this is a differentiating feature of these groups. Our study has also discovered that predictions of spectral tuning derived from studies of other vertebrates are of limited applicability to vipers, especially with respect to SWS1 and LWS visual pigments. In addition, we have found evidence of positive selection on regions of visual opsin genes that encode amino acids known to be of functional importance in chromophore binding (in *lws* and *rh1*) and spectral tuning (in *sws1* and *rh1*). Some of the questions raised by our study (especially about the distribution, polarity and function of potential viperine *versus* crotaline differences) can be tackled with broader and deeper studies of viper vision, but others will also benefit from more detailed studies of other groups of reptiles, especially other snakes. As hinted at by the anatomical studies of snake retinas by Gordon Walls and Garth Underwood, the evolutionary biology of snake vision is fertile ground for provocative research topics in snake and vision biology.

ACKNOWLEDGEMENTS

This work was supported by grants from the Leverhulme Trust (RPG-342 to DJG, NSH, DMH & JCP) and the Department of Life Sciences of The Natural History Museum, London. Permits for research and export were granted by Direction de l'Environment de l'Aménagement et du Logement and the Direction des Services Vétérinaires de la Guyane, Cayenne, French Guiana. For assistance in the field,

DJG thanks Gabriela Bittencourt-Silva, Antoine Fouquet, Philippe Gaucher, Jeannot and Odette (Camp Patawa) and Mark Wilkinson. Additional practical assistance with obtaining and processing samples, and with literature, analysis and discussion was provided by Gerlinde Heiß-Herzberger, Gay Kennaway, Robert Lubbersen, Sonja Meimann, David Nixon, Gill Sparrow, Ed Wade, Wolfgang Wüster, NHM Sequencing Facility, the Zoological Society of London, and especially Simon Maddock and David Richards. We thank KL Sanders and D Pisani for support. BFS is funded by a European Union H2020 – Marie Skłodowska-Curie Global Fellowship (GA703438). BFS and DMH are funded by a Australian Research Council Discovery (DP180101688). NLO's contribution was funded by the Russian Foundation of Basic Research 18-04-00040 and 19-04-00119. We thank Michele Menegon and David Richards for providing photographs of vipers in life. This article was improved by constructive criticism from two anonymous reviewers.

REFERENCES

Amemiya CT, Alföldi J, Lee AP, Fan S, Philippe H, Maccallum I, Braasch I, Manousaki T, Schneider I, Rohner N, Organ C, Chalopin D, Smith JJ, Robinson M, Dorrington RA, Gerdol M, Aken B, Biscotti MA, Barucca M, Baurain D, Berlin AM, Blatch GL , Buonocore F, Burmester T, Campbell MS, Canapa A, Cannon JP, Christoffels A, De Moro G, Edkins AL, Fan L, Fausto AM, Feiner N, Forconi M, Gamieldien J, Gnerre S, Gnirke A, Goldstone JV, Haerty W, Hahn ME, Hesse U, Hoffmann S, Johnson J, Karchner SI, Kuraku S, Lara M, Levin JZ, Litman GW, Mauceli E, Miyake T, Mueller MG, Nelson DR, Nitsche A, Olmo E, Ota T, Pallavicini A, Panji S, Picone B, Ponting CP, Prohaska SJ, Przybylski D, Saha NR, Ravi V, Ribeiro FJ, Sauka-Spengler T, Scapigliati G, Searle SMJ, Sharpe T, Simakov O, Stadler PF, Stegeman JJ, Sumiyama K, Tabbaa D, Tafer H, Turner-Maier J, van Heusden P, White S, Williams S, Yandell M, Brinkmann H. Volff J-N, Tabin C-J, Shubin N, Schartl M, Jaffe DB, Postlethwait JH, Venkatesh B, Di Palma F, Lander ES, Meyer A, Lindblad-Toh K. 2013. The African coelacanth genome provides insights into tetrapod evolution. *Nature* 496: 311–316.

Asenjo AB, Rim J, Oprian DD. 1994. Molecular determinants of human red/green color discrimination. *Neuron* 12: 1131–1138.

Berson DM, Hartline PH. 1988. A tecto-rotundo-telencephalic pathway in the rattlesnake: evidence for a forebrain representation of the infrared sense. *Journal of Neuroscience* 8: 1074–1088.

Bielawski JP, Yang Z. 2004. A maximum likelihood method for detecting functional divergence at individual codon sites, with application to gene family evolution. *Journal of Molecular Evolution* 59: 121–132.

Blanks JC, Johnson LV. 1984. Specific binding of peanut lectin to a class of retinal photoreceptor cells. A species comparison. *Investigative Ophthalmology & Visual Science* 25: 546–557.

Bullock TH, Diecke FP. 1956. Properties of an infra-red receptor. *The Journal of Physiology* 134: 47–87.

Burbrink FT, Guiher TJ. 2014. Considering gene flow when using coalescent methods to delimit lineages of North American pitvipers of the genus *Agkistrodon*. *Zoological Journal of the Linnean Society* 173: 505–526.

Burnside B. 2001. Light and circadian regulation of retinomotor movement. *Progress in Brain Research* 131: 477–485.

Cadle JE. 1992. Phylogenetic relationships among vipers: immunological evidence. In: Campbell JA, Brodie ED, eds. *Biology of pitvipers*. Tyler, USA, 41–48.

Carvalho LS, Cowing JA, Wilkie SE, Bowmaker JK, Hunt DM. 2007. The molecular evolution of avian ultraviolet- and violet-sensitive visual pigments. *Molecular Biology and Evolution* 24: 1843–1852.

Carvalho LS, Davies WL, Robinson PR, Hunt DM. 2011. Spectral tuning and evolution of primate short-wavelength-sensitive visual pigments. *Proceedings of the Royal Society B: Biological Sciences* 279: 387–393.

Castoe TA, de Koning APJ, Hall KT, Card DC, Schield DR, Fujita MK, Ruggiero RP, Degner JF, Daza JM, Gu W, *et al.* 2013. The Burmese python genome reveals the molecular basis for extreme adaptation in snakes. *Proceedings of the National Academy of Sciences of the United States of America* 110: 20645–20650.

Catania KC. 2011. The brain and behavior of the tentacled snake. *Annals of the New York Academy of Sciences* 1225: 83–89.

Catania KC, Remple FE. 2004. Tactile foveation in the star-nosed mole. *Brain, Behavior and Evolution* 63: 1–12.

Darriba D, Taboada GL, Doallo R, Posada D. 2012. jModelTest 2: more models, new heuristics and parallel computing. *Nature Methods* 9: 772.

Davies WIL, Collin SP, Hunt DM. 2012. Molecular ecology and adaptation of visual photopigments in craniates. *Molecular Ecology* 21: 3121–3158.

Davies WL, Cowing JA, Bowmaker JK, Carvalho LS, Gower DJ, Hunt DM. 2009. Shedding light on serpent sight: the visual pigments of henophidian snakes. *Journal of Neuroscience* 29: 7519–7525.

Fay JC, Wu CI. 2003. Sequence divergence, functional constraint, and selection in protein evolution. *Annual review of genomics and human genetics* 4: 213–235.

Fleishman LJ, Loew ER, Whiting MJ. 2011. High sensitivity to short wavelengths in a lizard and implications for understanding the evolution of visual systems in lizards. *Proceedings of the Royal Society B: Biological Sciences* 278: 2891–2899.

Gilad Y, Wiebe V, Przeworski M, Lancet D, Pääbo S. 2004. Loss of olfactory receptor genes coincides with the acquisition of full trichromatic vision in primates. *PLoS Biology* 2: 120–125.

Glosmann M, Steiner M, Peichl L, Ahnelt PK. 2008. Cone photoreceptors and potential UV vision in a subterranean insectivore, the European mole. *Journal of Vision* 8: 23–23.

Goris RC. 2011. Infrared organs of snakes: An integral part of vision. *Journal of Herpetology* 45: 2–15.

Goris RC, Terashima S. 1976. The structure and function of the infrared receptors of snakes. *Progress in Brain Research* 43: 159–170.

Govardovskii VI, Chkheidze NI. 1989. Retinal photoreceptors and visual pigments in certain snakes. *Biological Abstracts* 90: 1036.

Grace MS, Matshita A. 2007. Neural correlates of complex behavior: Vision and infrared imaging in boas and pythons. In: Henderson R & Powell R, *Biology of the Boas, Pythons and Related Taxa*. Utah: Eagle Mountain Publishing, 271–285.

Gracheva EO, Ingolia NT, Kelly YM, Cordero-Morales JF, Hollopeter G, Chesler AT, Sánchez EE, Perez JC, Weissman JS, Julius D. 2010. Molecular basis of infrared detection by snakes. *Nature* 464: 1006–1011.

Harrington SM, Reeder TW. 2017. Phylogenetic inference and divergence dating of snakes using molecules, morphology and fossils: new insights into convergent evolution of feeding morphology and limb reduction. *Biological Journal of the Linnean Society* 121: 379–394.

Hart NS, Coimbra JP, Collin SP, Westhoff G. 2012. Photoreceptor types, visual pigments, and topographic specializations in the retinas of hydrophiid sea snakes. *Journal of Comparative Neurology* 520: 1246–1261.

Hartline PH, Kass L, Loop MS. 1978. Merging of modalities in the optic tectum: infrared and visual integration in rattlesnakes. *Science* 199: 1225–1229.

Hauzman E, Bonci DMO, Grotzner SR, Mela M, Liber AMP, Martins SL, Ventura DF. 2014. Comparative study of photoreceptor and retinal ganglion cell topography and spatial resolving power in Dipsadidae snakes. *Brain, Behavior and Evolution* 84: 197–213.

Hauzman E, Bonci DMO, Suárez-Villota EY, Neitz M, Ventura DF. 2017. Daily activity patterns influence retinal morphology, signatures of selection, and spectral tuning of opsin genes in colubrid snakes. *BMC Evolutionary Biology* 17: 7519.

Hicks D, Molday RS. 1986. Differential immunogold dextran labeling of bovine and frog rod and cone cells using monoclonal-antibodies against bovine rhodopsin. *Experimental Eye Research* 42: 55–71.

Himsted W. 1996. *Die Blindwühlen*. Magdeburg, Germany: Westarp Wissenschaften.

Hirosawa K. 1978. A microscopic observation on the retina of habu, *Trimeresurus flavoviridis*. *Snake* 10: 20–23.

Hudson NJ, Baker ML, Hart NS, Wynne JW, Gu Q, Huang Z, Zhang G, Ingham AB, Wang L, Reverter A. 2014. Sensory rewiring in an echolocator: genome-wide modification of retinogenic and auditory genes in the bat *Myotis davidii*. *G3* 4: 1825–1835.

Hunt DM, Carvalho LS, Cowing JA, Parry JWL, Wilkie SE, Davies WL, Bowmaker JK. 2007. Spectral tuning of shortwave-sensitive visual pigments in vertebrates. *Photochemistry and Photobiology* 83: 303–310.

Jacobs G, II J, Tan Y, Li WH. 2002. Opsin gene and photopigment polymorphism in a prosimian primate. *Vision Research* 42: 11–18.

Jones G, Teeling EC, Rossiter SJ. 2013. From the ultrasonic to the infrared: molecular evolution and the sensory biology of bats. *Frontiers in Physiology* 4: 117.

Katoh K, Misawa K, Kuma K, Miyata T. 2002. MAFFT: a novel method for rapid multiple sequence alignment based on fast Fourier transform. *Nucleic Acids Research* 30: 3059–3066.

Khattab F, Khattab FI, Fares N. 2004. Retinal photoreceptor fine structure in some reptiles. *The Egyptian Journal of Hospital Medicine*: 167–186.

Krochmal AR. 2004. Heat in evolution's kitchen: evolutionary perspectives on the functions and origin of the facial pit of pitvipers (Viperidae: Crotalinae). *Journal of Experimental Biology* 207: 4231–4238.

Liu Y, Chen Q, Papenfuss TJ, Lu F, Tang Y. 2016. Eye and pit size are inversely correlated in crotalinae: Implications for selection pressure relaxation. *Journal of Morphology* 277: 107–117.

Loew ER. 1994. A third, ultraviolet-sensitive, visual pigment in the Tokay gecko (*Gekko gekko*). *Vision Research* 34: 1427–1431.

Loughran NB, Hinde S, McCormick-Hill S, Leidal KG, Bloomberg S, Loughran ST, O'Connor B, O'Fágáin C, Nauseef WM, O'Connell MJ. 2012. Functional consequence of positive selection revealed through rational mutagenesis of human myeloperoxidase. *Molecular Biology and Evolution 8: 2039–2046*.

Lythgoe JN. 1979. *The Ecology of Vision*. Oxford: Clarendon Press.

Mohun SM, Davies WL, Bowmaker JK, Pisani D, Himstedt W, Gower DJ, Hunt DM, Wilkinson M. 2010. Identification and characterization of visual pigments in caecilians (Amphibia:

Gymnophiona), an order of limbless vertebrates with rudimentary eyes. *Journal of Experimental Biology* 213: 3586–3592.

Moritz GL, Lim NTL, Neitz M, Peichl L, Dominy NJ. 2013. Expression and evolution of short wavelength sensitive opsins in colugos: A nocturnal lineage that informs debate on primate origins. *Evolutionary Biology* 40: 542–553.

Nathans J. 1990. Determinants of visual pigment absorbance: Role of charged amino acids in the putative transmembrane segments. *Biochemistry* 29: 937–942.

Newman EA, Hartline PH. 1981. Integration of visual and infrared information in bimodal neurons of the rattlesnake optic tectum. *Science* 213: 789–791.

Nießner C, Denzau S, Gross JC, Peichl L, Bischof HJ, Fleissner G, Wiltschko W, Wiltschko R. 2011. Avian ultraviolet/violet cones identified as probable magnetoreceptors. *PLoS ONE* 6: e20091.

Niven JE, Laughlin SB. 2008. Energy limitation as a selective pressure on the evolution of sensory systems. *Journal of Experimental Biology* 211: 1792–1804.

Odeen A, Hastad O. 2013. The phylogenetic distribution of ultraviolet sensitivity in birds. *BMC Evolutionary Biology* 13: 36.

Oelschläger HA. 1992. Development of the olfactory and terminalis systems in whales and dolphins. In: Doty RL, Müller-Schwarze D, eds. *Chemical Signals in Vertebrates 6*. Boston, MA: Springer, 141–147.

Pattengale ND, Alipour M, Bininda-Emonds ORP, Moret BME, Stamatakis A. 2010. How many bootstrap replicates are necessary? *Journal of Computational Biology* 17: 337–354.

Pettigrew JD, Manger PR, Fine SLB. 1998. The sensory world of the platypus. *Philosophical Transactions of the Royal Society B: Biological Sciences* 353: 1199–1210.

Phelps T. 2010. *Old World Vipers, A Natural History of the Azemiopinae and Viperinae*. Frankfurt am Main: Chimaira.

Pignatelli V, Champ C, Marshall J, Vorobyev M. 2010. Double cones are used for colour discrimination in the reef fish, *Rhinecanthus aculeatus*. *Biology Letters* 6: 537–539.

Pyron R, Burbrink FT, Wiens JJ. 2013. A phylogeny and revised classification of Squamata, including 4161 species of lizards and snakes. *BMC Evolutionary Biology* 13: 93.

Rasmussen JB. 1990a. The retina of *Psammodynastes pulverulentus* (Boie, 1827) and *Telescopus fallax* (Fleischmann, 1831) with a discussion of their phylogenetic significance (Colubroidea, Serpentes). *Journal of Zoological Systematics and Evolution* 28: 269–276.

Ronquist F, Teslenko M, van der Mark P, Ayres DL, Darling A, Hohna S, Larget B, Liu L, Suchard MA, Huelsenbeck JP. 2012. MrBayes 3.2: Efficient Bayesian phylogenetic inference and model choice across a large model space. *Systematic Biology* 61: 539–542.

Schiviz AN, Ruf T, Kuebber-Heiss A, Schubert C, Ahnelt PK. 2008. Retinal cone topography of artiodactyl mammals: influence of body height and habitat. *The Journal of Comparative Neurology* 507: 1336–1350.

Schleich CE, Vielma A, Glösmann M, Palacios AG, Peichl L. 2010. Retinal photoreceptors of two subterranean tuco-tuco species (Rodentia, *Ctenomys*): Morphology, topography, and spectral sensitivity. *The Journal of Comparative Neurology* 518: 4001–4015.

Schott RK, Refvik SP, Hauser FE, Lopez-Fernandez H, Chang BSW. 2014. Divergent positive selection in rhodopsin from lake and riverine cichlid fishes. *Molecular Biology and Evolution* 31: 1149–1165.

Schott RK, Müller J, Yang CGY, Bhattacharyya N, Chan N, Xu M, Morrow JM, Ghenu AH, Loew ER, Tropepe V, *et al.* 2016. Evolutionary transformation of rod photoreceptors in the all-cone retina of a diurnal garter snake. *Proceedings of the National Academy of Sciences of the United States of America* 113: 356-361.

Shi Y, Yokoyama S. 2003. Molecular analysis of the evolutionary significance of ultraviolet vision in vertebrates. *Proceedings of the National Academy of Sciences of the United States of America* 100: 8308–8313.

Sillman AJ, Govardovskii VI, Rohlich P, Southard JA, Loew ER. 1997. The photoreceptors and visual pigments of the garter snake (*Thamnophis sirtalis*): a microspectrophotometric, scanning electron microscopic and immunocytochemical study. *Journal of Comparative Physiology A* 181: 89–101.

Sillman AJ, Carver JK, Loew ER. 1999. The photoreceptors and visual pigments in the retina of a boid snake, the ball python (*Python regius*). *Journal of Experimental Biology* 202: 1931–1938.

Sillman AJ, Johnson JL, Loew ER. 2001. Retinal photoreceptors and visual pigments in *Boa constrictor imperator*. *Journal of Experimental Zoology* 290: 359–365.

Simões BF, Sampaio FL, Jared C, Antoniazzi MM, Loew ER, Bowmaker JK, Rodriguez A, Hart NS, Hunt DM, Partridge JC, *et al.* 2015. Visual system evolution and the nature of the ancestral snake. *Journal of Evolutionary Biology* 28: 1309–1320.

Simões BF, Sampaio FL, Loew ER, Sanders KL, Fisher RN, Hart NS, Hunt DM, Partridge JC, Gower DJ. 2016a. Multiple rod-cone and cone-rod photoreceptor transmutations in snakes: evidence from visual opsin gene expression. *Proceedings of the Royal Society B: Biological Sciences* 283: 20152624

Simões BF, Sampaio FL, Douglas RH, Kodandaramaiah U, Casewell NR, Harrison RA, Hart NS, Partridge JC, Hunt DM, Gower DJ. 2016b. Visual pigments, ocular filters and the evolution of snake vision. *Molecular Biology and Evolution* 33: 2483–2495.

Soares D, Niemiller ML. 2013. Sensory adaptations of fishes to subterranean environments. *BioScience* 63: 274–283.

Solovei I, Kreysing M, Lanctôt C, Kösem S, Peichl L, Cremer T, Guck J, Joffe B. 2009. Nuclear architecture of rod photoreceptor cells adapts to vision in mammalian evolution. *Cell* 137: 356–368.

Stamatakis A. 2014. RAxML version 8: a tool for phylogenetic analysis and post-analysis of large phylogenies. *Bioinformatics* 30: 1312–1313.

Steinberg RH, Reid M, Lacy PL. 1973. The distribution of rods and cones in the retina of the cat (*Felis domesticus*). *The Journal of Comparative Neurology* 148: 229–248.

Tan Y, Li WH. 1999. Trichromatic vision in prosimians. *Nature* 402: 36.

Terashima SI, Goris RC. 1975. Tectal organization of pit viper infrared reception. *Brain research* 83: 490–494.

Underwood G. 1967a. *A Contribution to the Classification of Snakes*. British Museum Natural History Publications.

Underwood G. 1970. The Eye. In: Gans C & Parsons TS, eds. *Biology of the Reptilia: Morphology B*. New York: Academic Press, 1–97.

Underwood G. 1997. An overview of venomous snake evolution. In: Thorpe RS, Wüster W and Malhotra A, eds. *Venomous snakes: Ecology, evolution and snakebite*. Oxford: Clarendon Press, 1–13.

van Doorn K, Sivak JG. 2015. Spectral transmittance of the spectacle scale of snakes and geckos. *Contributions to Zoology* 8: 1–12.

van Hazel I, Sabouhanian A, Day L, Endler JA, Chang BSW. 2013. Functional characterization of spectral tuning mechanisms in the great bowerbird short-wavelength sensitive visual pigment (SWS1), and the origins of UV/violet vision in passerines and parrots. *BMC Evolutionary Biology* 13: 250.

Veilleux CC, Bolnick DA. 2009. Opsin gene polymorphism predicts trichromacy in a cathemeral lemur. *American Journal of Primatology* 71: 86–90.

Walls GL. 1931. The occurrence of colored lenses in the eyes of snakes and squirrels, and their probable significance. *Copeia* 1931: 125–127.

Walls GL. 1942. *The Vertebrate Eye and Its Adaptive Radiation*. New York: Fafner Publishing Company.

Wang YS, Macke JP, Merbs SL, Zack DJ, Klauberg B, Bennett J, Gearhart J, Nathans J. 1992. A locus-control region adjacent to the human red and green visual pigment genes. *Neuron* 9: 429–440.

Weadick CJ, Chang BS. 2011. An improved Likelihood Ratio Test for detecting site-specific functional divergence among clades of protein-coding genes. *Molecular Biology and Evolution* 29: 1297–1300.

Weadick CJ, Chang BS. 2012. Complex patterns of divergence among green-sensitive (RH2a) African cichlid opsins revealed by Clade model analyses. *BMC Evolutionary Biology* 12: 206.

Wilkie SE, Robinson PR, Cronin TW, Poopalasundaram S, Bowmaker JK, Hunt DM. 2000. Spectral tuning of avian violet- and ultraviolet-sensitive visual pigments. *Biochemistry* 39: 7895–7901.

Wüster W, Peppin L, Pook CE, Walker DE. 2008. A nesting of vipers: Phylogeny and historical biogeography of the Viperidae (Squamata: Serpentes). *Molecular Phylogenetics and Evolution* 49: 445–459.

Yang Z. 2007. PAML 4: Phylogenetic analysis by maximum likelihood. *Molecular Biology and Evolution* 24: 1586–1591.

Yang ZH, Nielsen R, Goldman N, Pedersen A. 2000. Codon-substitution models for heterogeneous selection pressure at amino acid sites. *Genetics* 155: 431–449.

Yang ZH, Wong W, Nielsen R. 2005. Bayes Empirical Bayes inference of amino acid sites under positive selection. *Molecular Biology and Evolution* 22: 1107–1118.

Yoder AD, Chan LM, Reis dos M, Larsen PA, Campbell CR, Rasolarison R, Barrett M, Roos C, Kappeler P, Bielawski J, Yang Z. 2014. Molecular evolutionary characterization of a V1R subfamily unique to strepsirrhine primates. *Genome Biology and Evolution 6:213-227*.

Yokoyama S. 2000. Molecular evolution of vertebrate visual pigments. *Progress in Retinal and Eye Research* 19: 385–419.

Yokoyama S. 2008. Evolution of dim-light and color vision pigments. *Annual Review of Genomics and Human Genetics* 9: 259–282.

Yokoyama S, Starmer WT, Takahashi Y, Tada T. 2006. Tertiary structure and spectral tuning of UV and violet pigments in vertebrates. *Gene* 365: 95–103.

Yokoyama S, Tada T, Zhang H, Britt L. 2008. Elucidation of phenotypic adaptations: Molecular analyses of dim-light vision proteins in vertebrates. *Proceedings of the National Academy of Sciences* 105: 13480–13485.

Zhang J, Nielsen R, Yang Z. 2005. Evaluation of an improved branch-site likelihood method for detecting positive selection at the molecular Level. *Molecular Biology and Evolution* 22: 2472–2479.

Zhao H, Rossiter SJ, Teeling EC, Li C, Cotton JA, Zhang S. 2009a. The evolution of color vision in nocturnal mammals. *Proceedings of the National Academy of Sciences of the United States of America* 106: 8980–8985.

Zhao H, Ru B, Teeling EC, Faulkes CG, Zhang S, Rossiter SJ. 2009b. Rhodopsin molecular evolution in mammals inhabiting low light environments. *PLoS ONE* 4: e8326.

SUPPORTING INFORMATION

Additional supporting information may be found in the online version of this article at the publisher's website:

Table S1. Identification and GenBank accession numbers of the samples used in this study. Sequences newly generated for this study are indicated in bold.

Table S2. Known amino-acid spectral tuning sites for *sws1* (Yokoyama et al. 2006) and predicted peak absorbance (λ_{max}) for vipers. Site values in first row represent amino-acid positions numbered with respect to bovine rhodopsin. Underline indicates amino acids with stronger effects on spectral tuning (Cowing *et al.*, 2002; Babu *et al.*, 2001; Asenjo *et al.*, 1994 and Fasick *et al.*, 2002). All λ_{max} values are predicted (for a review see Yokoyama, 2008; see also comments by Simões et al., 2016) based on amino-acid sequences except those in parentheses (measured using MSP). UVS = ultraviolet sensitive (λ_{max} ca. 360 nm). Data for *Bitis nasicornis, Echis ocellatus* and *Causus rhombeatus* from Simões et al. (2016). * = different specimens of this species were subjected to opsin gene sequencing and MSP. † = Simões et al. (2016) did not predict an Lmax for these species because of uncertainty about the functional consequence of the combination of amino acids at these tuning sites; however, additional viperid MSP data reported here indicates that tuning site 93 does not seem to play a major role in determining whether the SWS1 pigment is UVS or not, with site 86 perhaps being more influential (as in mammals: Hunt et al. 2009, Hauser et al. 2014).

Table S3. Known amino-acid spectral tuning sites for *rh1* (Yokoyama *et al.*, 2008; Hunt *et al.*, 2001) and predicted peak absorbance (λ_{max}) for squamates. Site values in first row represent amino-acid positions numbered with respect to bovine rhodopsin. All λ_{max} values are predicted (for a review see Yokoyama *et al.*, 2008; see also comments by Simões et al., 2016) based on amino-acid sequences except those in parentheses (measured using MSP). Data for *Bitis nasicornis, Echis ocellatus* and *Causus rhombeatus* from Simões et al. (2016). * = different specimens of this species were subjected to opsin gene sequencing and MSP. a = data from Govardovskii & Chkheidze (1989).

Table S4. Known amino-acid spectral tuning sites for *lws* (Yokoyama and Radlwimmer, 1998) and predicted peak absorbance (λ_{max}) for squamates. Site values in first row represent amino-acid positions numbered with respect to bovine rhodopsin. Underline indicates amino acids with stronger effects on spectral tuning (Cowing *et al.*, 2002; Babu *et al.*, 2001; Asenjo *et al.*, 1994 and Fasick *et al.*, 2002). All λ_{max} values are predicted (for a review see Yokoyama, 2008; see also comments by Simões et al., 2016) based on amino-acid sequences except those in parentheses (measured using MSP). Data for *Bitis nasicornis, Echis ocellatus* and *Causus rhombeatus* from Simões et al. (2016). * = different specimens of this species were subjected to opsin gene sequencing and MSP. a = data from Govardovskii & Chkheidze (1989).

Table S5. Ratio of synonymous to non-synonymous substitutions (dN/dS = ω) for snake visual opsin gene sequences under branch models. 2Δl = twice the difference logarithm of the likelihood value for the models.

Table S6. Ratio of synonymous to non-synonymous substitutions (dN/dS = ω) for snake visual opsin gene sequences under site models. For each gene two pairs of models are

compared to test for significant difference in goodness-of-fit to data. 2Δl = twice the difference logarithm of the likelihood value for the models.

Table S7. Amino acid sites inferred to be under positive selection (using Bayes Empirical Bayes), identified under site models for the three visual opsin genes in snakes (including vipers). Sites in bold are those known to be associated with spectral tuning of the corresponding visual pigment and those marked with an asterisk are associated with stabilization of the chromophore (retinal) pocket.

Table S8. Amino acid sites inferred to be under positive selection (using Bayes Empirical Bayes), identified under branch-site models for the three visual opsin genes in pit vipers (Crotalinae) (foreground branch) among all snakes.

Table S9. Clade model C (CMC) PAML analysis of visual opsin gene sequences in snakes partitioned by IR-detecting pit vipers (Crotalinae) versus other snakes.

Table S10. Ratio of synonymous to non-synonymous substitutions (dN/dS = ω) for viperid visual opsin gene sequences under branch models. 2Δl = twice the difference logarithm of the likelihood value for the models.

Table S11. Ratio of synonymous to non-synonymous substitutions (dN/dS = ω) for viperid visual opsin gene sequences under site models. For each gene two pairs of models are compared to test for significant difference in goodness-of-fit to data. 2Δl = twice the difference logarithm of the likelihood value for the models.

Table S12. Amino acid sites inferred to be under positive selection (using Bayes Empirical Bayes), identified under site models for the three visual opsin genes in viperid snakes. Sites in bold are those known to be associated with spectral tuning of the corresponding visual

pigment and those marked with an asterisk are associated with stabilization of the chromophore (retinal) pocket.

Table S13. Amino acid sites inferred to be under positive selection (using Bayes Empirical Bayes), identified under branch-site models for the three visual opsin genes in particular lineages (foreground branch) in viperids. Sites in bold are those known to be associated with spectral tuning.

Table S14. Clade model C (CMC) PAML analysis of visual opsin gene sequences in viperids partitioned by IR-detecting pit vipers (Crotalinae) versus other viperids (Viperinae and Azemiopinae).

Figure S1. Maximum Likelihood rhodopsin 1 (*rh1*) gene phylogenetic tree for squamates estimated by RAxML based on GTR+G+I model of sequence evolution. Black circles on internal branches indicate ML bootstrap support and Bayesian posterior probabilities above or equal to 80% and 1, respectively.

Figure S2. Maximum Likelihood short-wavelength opsin 1 (*sws1*) gene phylogenetic tree for squamates estimated by RAxML based on GTR+G+I model of sequence evolution. Black circles on internal branches indicate ML bootstrap support and Bayesian posterior probabilities above or equal to 80% and 1, respectively. SV = splice variant.

Figure S3. Maximum Likelihood medium-to-long wavelength opsin gene (*lws*) phylogenetic tree for squamates estimated by RAxML based on GTR+G+I model of sequence evolution. Black circles on internal branches indicate ML bootstrap support and Bayesian posterior probabilities above or equal to 80% and 1, respectively.

FIGURE CAPTIONS

Figure 1. Spectral absorbance measured by MSP for SWS1 (crosses), RH1 (empty circles) and LWS (filled diamonds) for three viper species. Plotted points are overlain with a vitamin-A_1 (rhodopsin) visual pigment template (lines). Spectral transmittance (lower right) of lenses and spectacles (brilles) of three viper species.

Figure 2. Viper phylogeny (from Pyron *et al.*, 2013; though following Wüster *et al.*, 2008 for relationships among *Echis, Causus* and *Cerastes*) showing estimated (on branches) and measured (in values under species name) λ_{max} for the three visual opsins detected. Estimated λ_{max} values are predictions made from cDNA sequences following 'known' effects of amino acid substitutions at spectral tuning sites in other vertebrates (see text). Measured values are from MSP studies: (#) (Govardovskii & Chkheidze, 1989) and (*) this study. Photographs at right of figure show heads in approximately left lateral view of (from top to bottom) the viperine *Vipera berus*, the azemiopine *Azemiops kharini,* and the crotaline *Crotalus durissus* (a pit viper – note IR-sensing pit between and slightly below eye and nostril). Photographs by M. Menegon, N Orlov and D Richards, respectively. Note that our MSP data are for *C. atrox*, whereas our opsin sequence data are for *C. durissus* (see Supporting Information, Table S1).

Figure 3. Light microscopic images of semithin sections of the retina of *Bitis arietans.* Upper left: Radial section of the retina. The outer retina shows two tiers of photoreceptors: Long single cone inner segments (LSC IS) in the outer tier, and rods (RIS ROS) and short single cones SSC) in the inner tier. Double cones were not identified unequivocally. The number of

somata in the inner nuclear layer outnumbers the photoreceptor somata by a factor of about 1.6:1.

Upper right: Tangential section of the photoreceptor layer. The left half shows many short single cone inner segments (SSC IS) surrounding the paler rod outer segments (ROS). In the transition between the inner and outer tier (right) the inner segment of the long single cone (LSC IS) starts to appear in the centre of the circular bead-like pattern of the short single cone inner segments. The right part of the micrograph is dominated by the inner segments of the large single cones (LSC IS) and occasional apical processes of the retinal pigment epithelium (RPE).

Lower left: Electron micrograph of the outer plexiform layer with a single one pedicle SC CP) containing many synaptic ribbons (sr) and several smaller rod spherules (RS).

Lower right: Electron micrograph of short and long single cone inner segments (SSC IS, LSC IS) highlighting the presence of numerous mitochondria (m).

Figure 4. Light microscope images of semithin sections of the retina of *Echis coloratus.*

Upper left: Radial section of the entire retina. There are about as many somata in the outer as in the inner nuclear layer. GCL ganglion cell layer, INL inner nuclear layer, IPL inner plexiform layer, LSC IS inner segments of long single cones, LSC OS outer segments of long single cones, OLM outer limiting membrane, ONL outer nuclear layer, OPL outer plexiform layer, RPE retinal pigment epithelium, RIS rod inner segments, ROS rod outer segments, SSC short single cones

Upper middle: Outer retina, radial section. The photoreceptors are arranged in two tiers: The scleral-most layer contains inner and outer segments of long single cones (LSC IS, LSC

OS). The innermost layer contains numerous rods (RIS ROS) as well as sparser short single cones (SSC IS, SSC OS.

Upper right: Tangential section of the outer retina. The upper left shows inner segments of long single cones (LSC) corresponding to the outer layer, and the lower right is dominated by many uniform rod outer segments (ROS) and several short single cone inner segments (SSC IS).

Lower left: Electron micrograph of the scleral region of the outer plexiform layer showing numerous rod spherules (RS) each containing one or two synaptic ribbons (sr, tangential view)

Lower right: Electron micrograph of a single cone pedicle (SC CP) in radial view characterized by numerous ribbon synapses (sr). Two rod spherules (RS) are seen more sclerad, with one or two ribbons (sr).

Figure 5. Viper retinas immunolabelled for rod opsin. Transverse sections of *Echis coloratus* (a, b) and *Crotalus durissus* (c, d). Both species show strong labelling of rod outer segments and possess high-density populations of rods (a, c). Overexposure shows that the rod inner segments, somata in the ONL and synaptic endings (rod spherules) in the OPL also are faintly labelled (b, d). This is particularly obvious in *E. coloratus* (b), where the rod somata extend throughout the thickness of the ONL (b). In *C. durissus* some rods are more strongly labelled than the remainder and stand out in isolation (d). Frames (b) and (d) show parts of frames (a) and (c), respectively. The scale bar in (a) applies to all images.

Figure 6. Immunolabelling of cones in *Echis coloratus* retinal transverse sections. (a1) Section double-labelled for PNA (LWS cones, green) and SWS1 opsin (magenta), there is no

colocalisation of both labels in any cones (which would appear white). Labelled cone outer segments are located in two tiers, an inner tier containing regular LWS and SWS1 cone outer segments and an outer tier containing exclusively external LWS cone outer segments. (a2) same field seen in differential interference contrast (DIC) to show the general morphology; the fat inner segments of external cones are located distal of the outer segments of the regular cones and rods; remains of dark retinal pigment epithelium are attached to the outer segments of the external cones. (a3) Superposition of (a1) and (a2) to show the localization of the opsin label in the outer segments; the arrow indicates an LWS double cone. (b1) Section double-labelled for PNA (green) and SWS1 opsin (magenta), there is no colocalisation of the two labels; (b2) DIC image of the same field, showing the fat cone inner segments between the slender rod inner segments; (b3) superposition of (b1) and (b2), labelled cone outer segments are attached to fat inner segments. The arrows indicate an LWS and an SWS1 double cone, the accessory members of these double cones have more slender inner segments than the principal members. (c1-2) Section double-labelled for LWS opsin (green) and PNA (red) to show that all LWS cones and only LWS cones are labelled by PNA. The two labels colocalise in the LWS cone outer segments. (c3) Superposition of a DIC image of the same field with the labels, showing that LWS cone outer segments are attached to fat inner segments. ext-L, external (outer) LWS cones. The magnification of the three series differs, each series (a, b, c) has its own scale bar.

Figure 7. Immunolabelling of cones in *Crotalus durissus* retinal transverse sections. (a1) Section double-labelled for LWS opsin (green) and SWS1 opsin (magenta), there is no coexpression of both opsins in any cones (which would appear white); (a2) same field seen in differential interference contrast (DIC) to show the general morphology, remains of dark

retinal pigment epithelium are attached to the photoreceptor outer segments; (a3) superposition of (a1) and (a2) to show the localization of the opsin label in the outer segments. (b1) Section double-labelled for PNA (LWS cone marker, green) and SWS1 opsin (magenta), there is no colocalisation of the two labels; (b2) DIC image of the same field, showing the fat cone inner segments between the slender rod inner segments; (b3) superposition of (b1) and (b2), labelled cone outer segments are attached to fat inner segments. (c1) Section double-labelled for LWS opsin (green) and PNA (magenta) to show that all LWS cones and only LWS cones are labelled by PNA. LWS opsin is located more distally and PNA more proximally in the LWS cone outer segments; (c2) DIC image of the same field, showing the fat cone inner segments; (c3) superposition of (c1) and (c2), labelled LWS cone outer segments are attached to fat inner segments. The magnification of the three series differs, each series (a, b, c) has its own scale bar.

Figure 8. Cone photoreceptor populations in viper retinas. Double immunofluorescence labelling for LWS and SWS1 opsin in flat-mounted retinas, the focus is on the opsin-containing cone outer segments. Cone density is much higher in *C. durissus* than in *E. coloratus*, the SWS1 cones form a minority in both species, and the merge of the two fluorescence channels shows that the LWS and SWS1 cones form separate populations, there is no coexpression of the two opsins in any cones (such cones would appear white). The images are maximum intensity projections of confocal image stacks, the few white structures in the *C. durissus* merged image are instances where outer segments lie on top of each other. For *E. coloratus*, three LWS double cones are marked by arrow heads. Because of the lower cone density, the *E. coloratus* images are displayed at lower magnification to show

a larger field. Note that the cone outer segments are considerably larger in *E. coloratus* than in *C. durissus* (c.f. Figs. 6b, 7b, 9)

Figure 9. Examples of double cones in *Echis coloratus* (a-f) and *Crotalus durissus* (g-l). (a) LWS double cone with a fat inner segment of the principal cone and a slender, shorter inner segment of the accessory cone; (a1) PNA label, (a2) DIC image of the same field, (a3) superposition of (a1) and (a2). (b) LWS double cone (right) and SWS1 single cone (left); the inner segment of the LWS accessory member is more slender than that of the LWS principal member, the inner segment of the SWS1 cone is smaller than that of the LWS principal cone; (b1) double-labelling for LWS opsin (green) and SWS1 opsin (magenta), (b2) DIC image of the same field, (b3) superposition of (b1) and (b2). (c-f) examples of LWS double cones (c, d) and SWS1 double cones (e, f) from flat-mounted retina, only the opsin-containing outer segments are shown. (g) LWS double cone (left) and LWS single cone (right), both with fat inner segments; (g1) double labelling of LWS cones (LWS opsin in green, PNA in magenta), (g2) DIC image of the same field, (g3) superposition of (g1) and (g2). (h) LWS double cone with relatively slender inner segments; (h1) double labelling for LWS opsin (green) and PNA (magenta), (h2) DIC image of the same field, (h3) superposition of (h1) and (h2). (i-k) examples of LWS double cones (arrowheads), (l) a potential SWS1 double cone; from flat-mounted retina, only the opsin-containing outer segments are shown. (a, b, g, h) are single focal images from retinal transverse sections, (c-f, i-l) are maximum intensity projections of confocal image stacks from flat-mounted retinas (c.f. Fig. 8). The scale bar in (a1) applies to all images. Note that the cone outer segments are considerably larger in *E. coloratus* than in *C. durissus*.

Figure 10. Photoreceptor mosaics in viper retinas. DIC images at the level of the photoreceptor inner segments in flat-mounted retinas. (a) *C. durissus*, showing the regular mosaic of the larger cone inner segments (one marked by an arrowhead); in the centre, the smaller profiles of the rod inner segments are also in focus. (b) *E. coloratus*, showing the dense cobblestone-like mosaic of the rods, presumably also including the small single cones. A few interspersed larger out-of-focus profiles presumably are the inner segments of large single cones (three marked by arrowheads). The scale bar in (b) applies to both images.

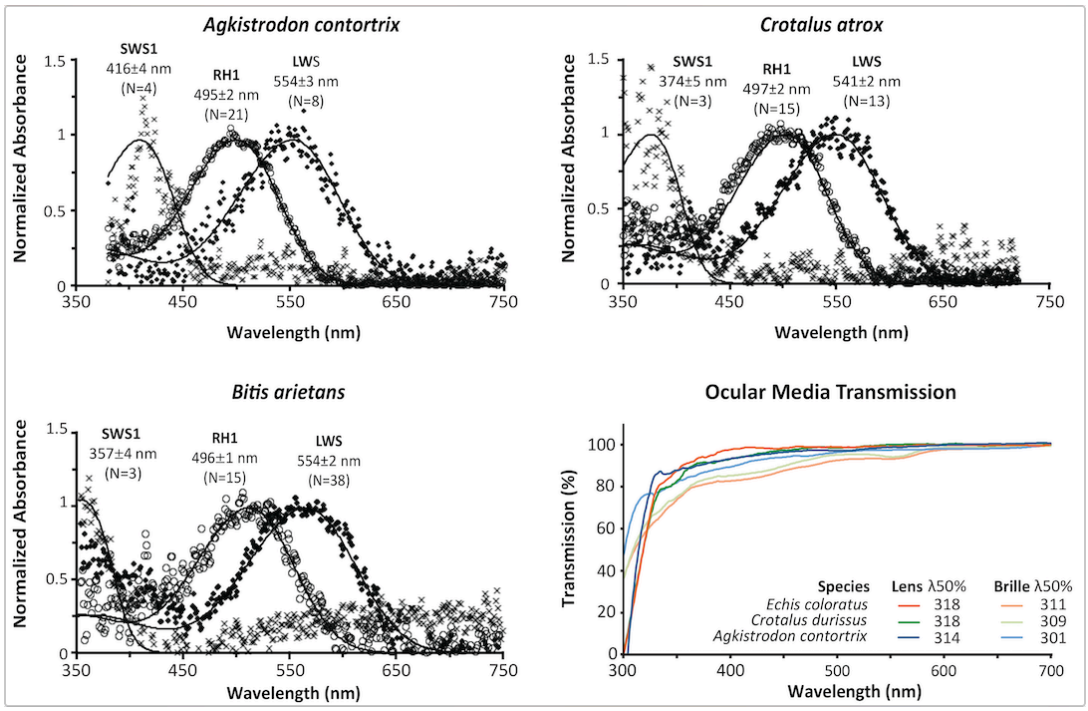
Agkistrodon contortrix
SWS1
416±4 nm
(N=4)
RH1
495±2 nm
(N=21)
LWS
554±3 nm
(N=8)
Normalized Absorbance
Wavelength (nm)
Crotalus atrox
SWS1
374±5 nm
(N=3)
RH1
497±2 nm
(N=15)
LWS
541±2 nm
(N=13)
Bitis arietans
SWS1
357±4 nm
(N=3)
RH1
496±1 nm
(N=15)
LWS
554±2 nm
(N=38)
Ocular Media Transmission
Transmission (%)
Species
Lens λ50%
Brille λ50%
Echis coloratus
318
311
Crotalus durissus
318
309
Agkistrodon contortrix
314
301

Fig. 1

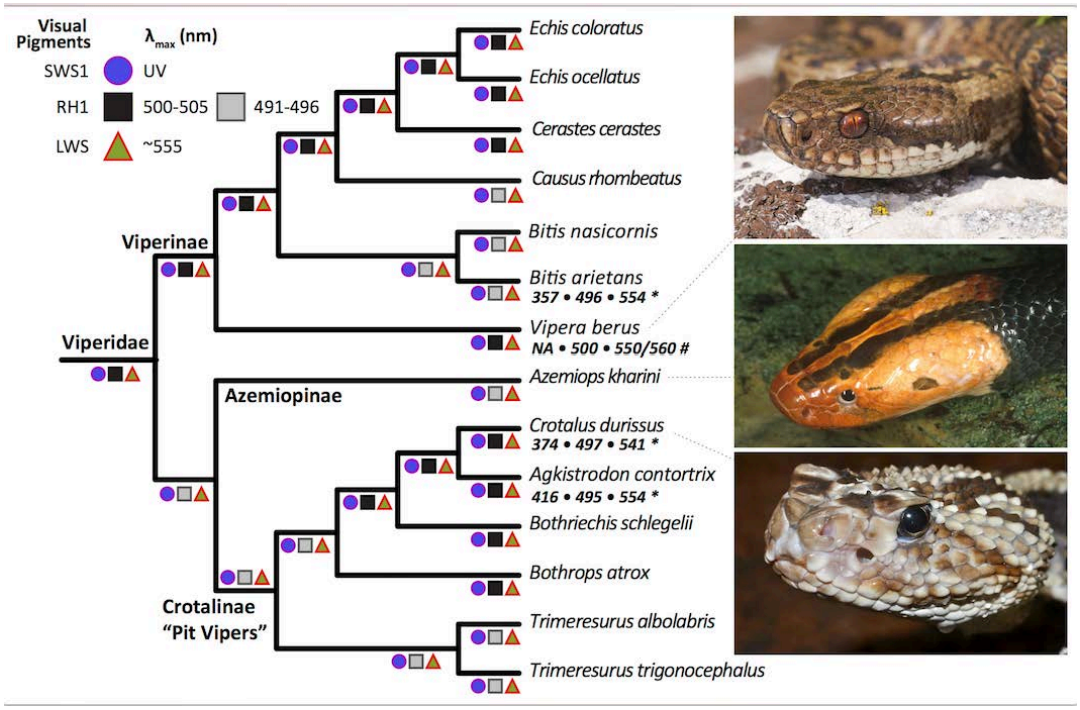
Visual Pigments
λmax (nm)
SWS1
UV
RH1
500-505
491-496
LWS
~555
Viperinae
Viperidae
Azemiopinae
Crotalinae
"Pit Vipers"
Echis coloratus
Echis ocellatus
Cerastes cerastes
Causus rhombeatus
Bitis nasicornis
Bitis arietans
357 • 496 • 554 *
Vipera berus
NA • 500 • 550/560 #
Azemiops kharini
Crotalus durissus
374 • 497 • 541 *
Agkistrodon contortrix
416 • 495 • 554 *
Bothriechis schlegelii
Bothrops atrox
Trimeresurus albolabris
Trimeresurus trigonocephalus

Fig. 2

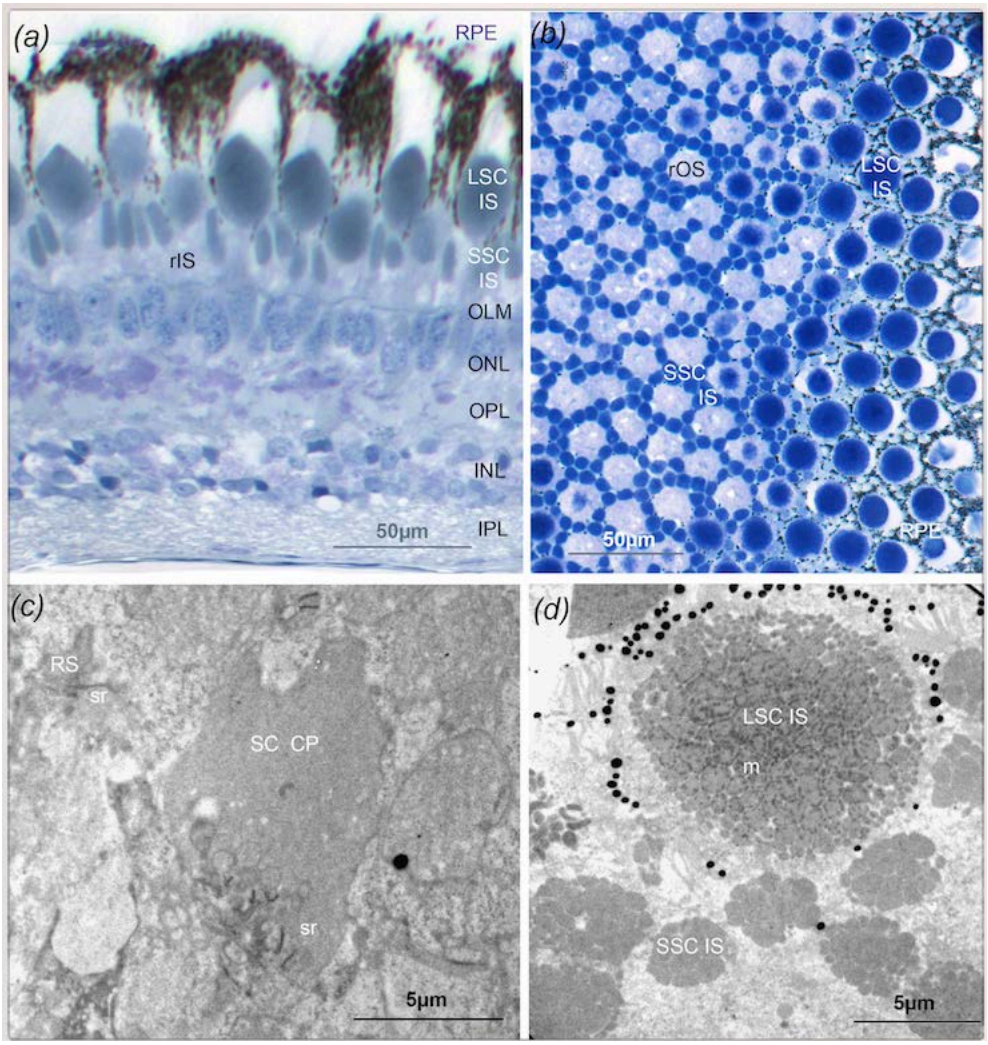
(a)
RPE
LSC IS
rIS
SSC IS
OLM
ONL
OPL
INL
50μm
IPL
(b)
rOS
LSC IS
SSC IS
50μm
RPE
(c)
RS
sr
SC CP
sr
5μm
(d)
LSC IS
m
SSC IS
5μm

Fig. 3

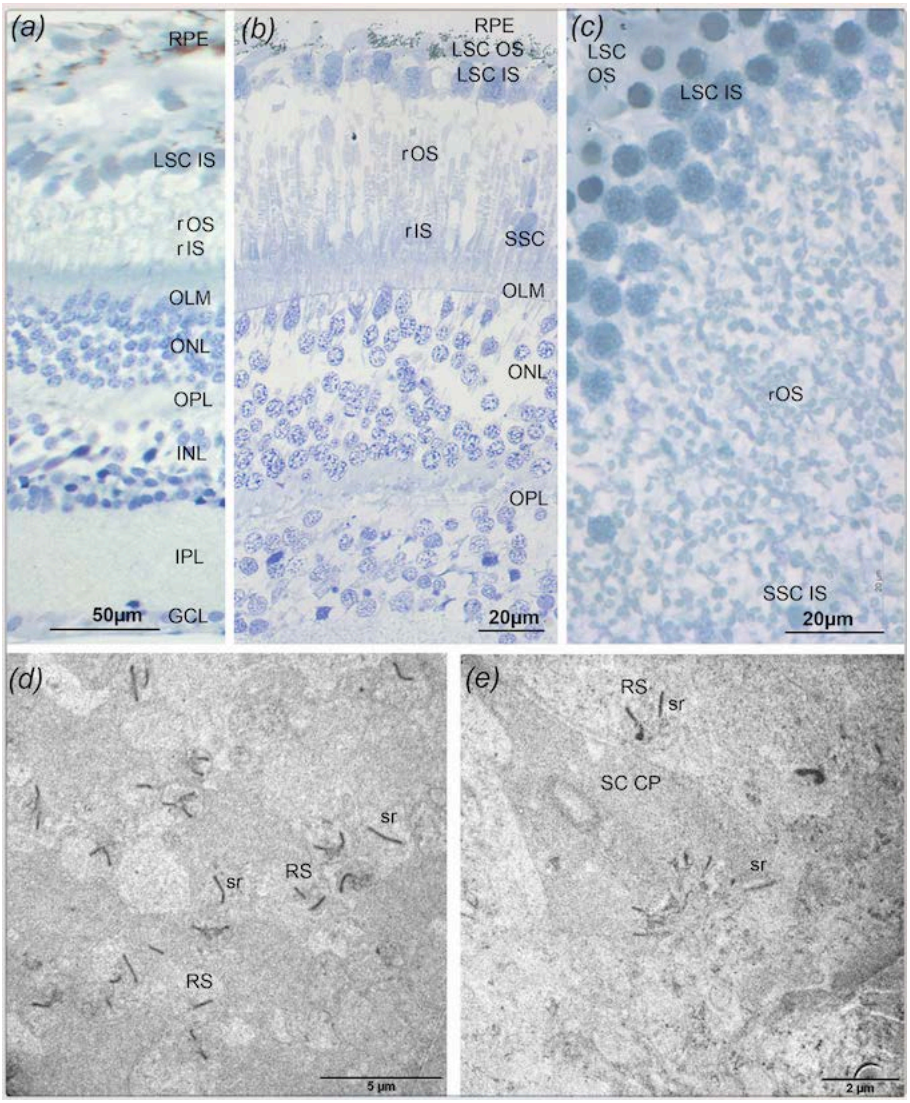
(a)
RPE
LSC IS
rOS
rIS
OLM
ONL
OPL
INL
IPL
50µm
GCL
(b)
RPE
LSC OS
LSC IS
rOS
rIS
SSC
OLM
ONL
OPL
20µm
(c)
LSC
OS
LSC IS
rOS
SSC IS
20µm
(d)
sr
sr
RS
RS
5 µm
(e)
RS
sr
SC CP
sr
2 µm

Fig. 4

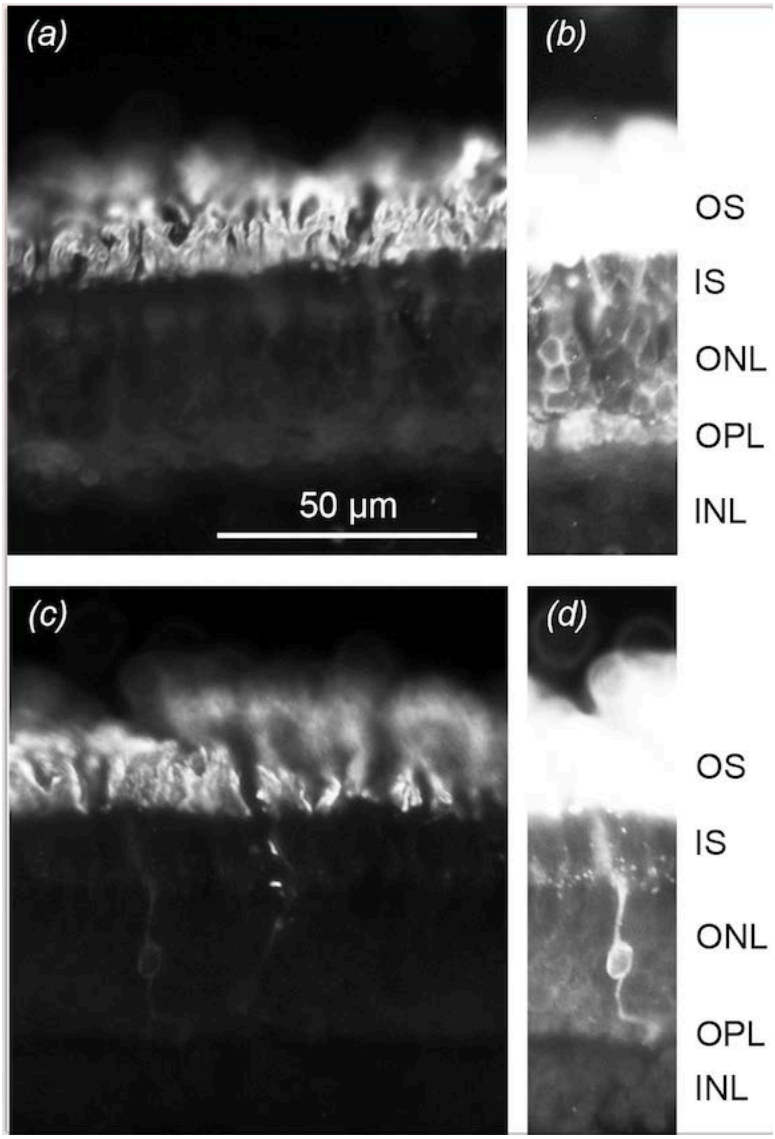

Fig. 5

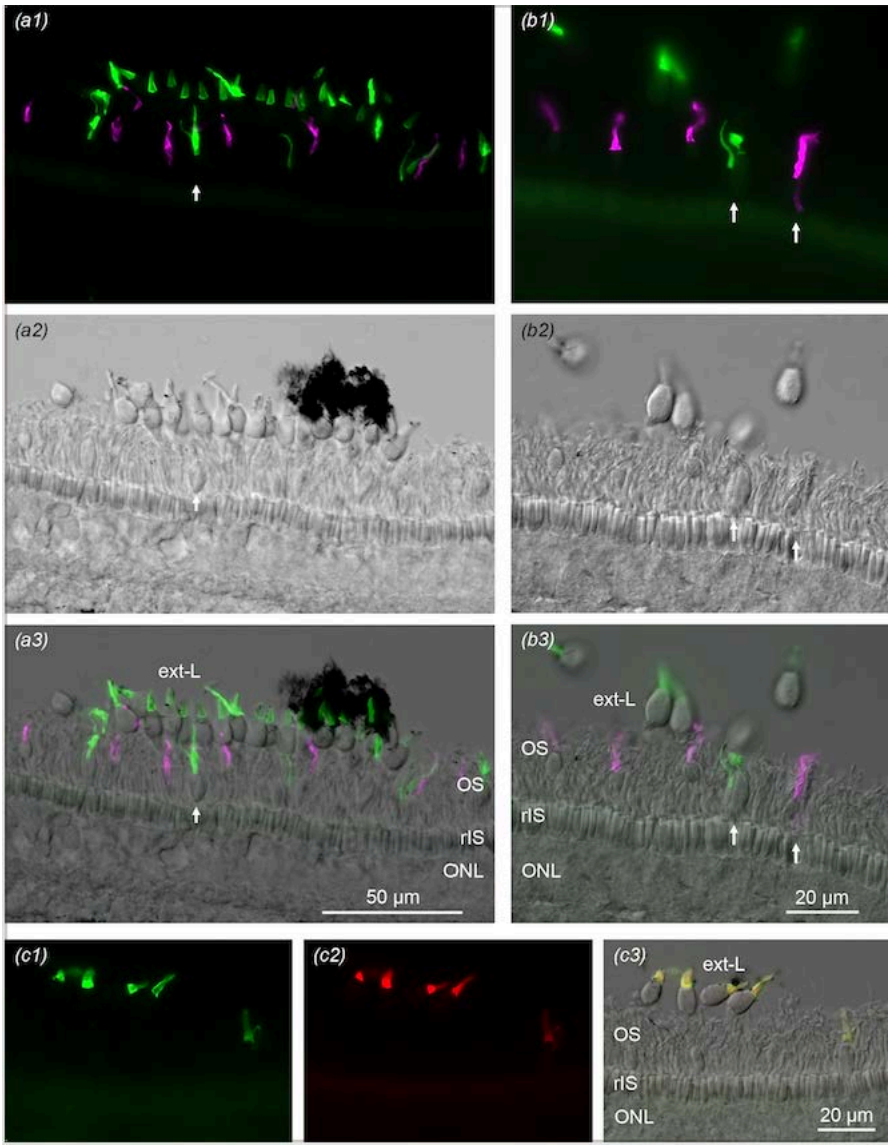
(a1)
(b1)
(a2)
(b2)
(a3)
ext-L
OS
rIS
ONL
50 µm
(b3)
ext-L
OS
rIS
ONL
20 µm
(c1)
(c2)
(c3)
ext-L
OS
rIS
ONL
20 µm

Fig. 6

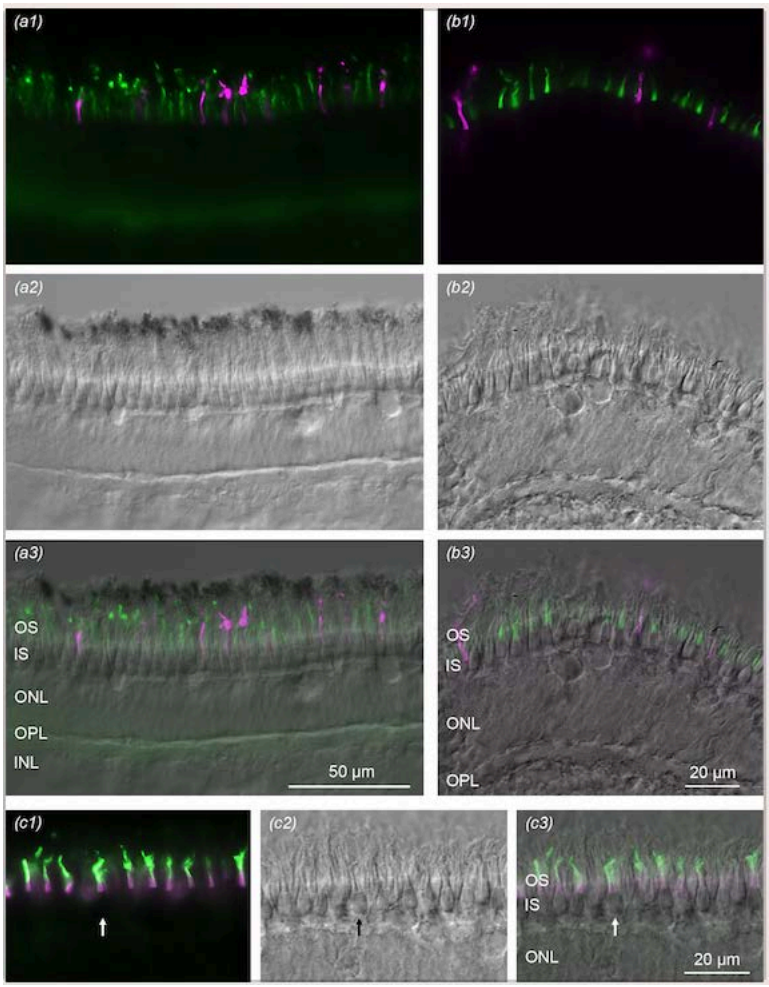
(a1)
(b1)
(a2)
(b2)
(a3)
OS
IS
ONL
OPL
INL
50 µm
(b3)
OS
IS
ONL
OPL
20 µm
(c1)
(c2)
(c3)
OS
IS
ONL
20 µm

Fig. 7

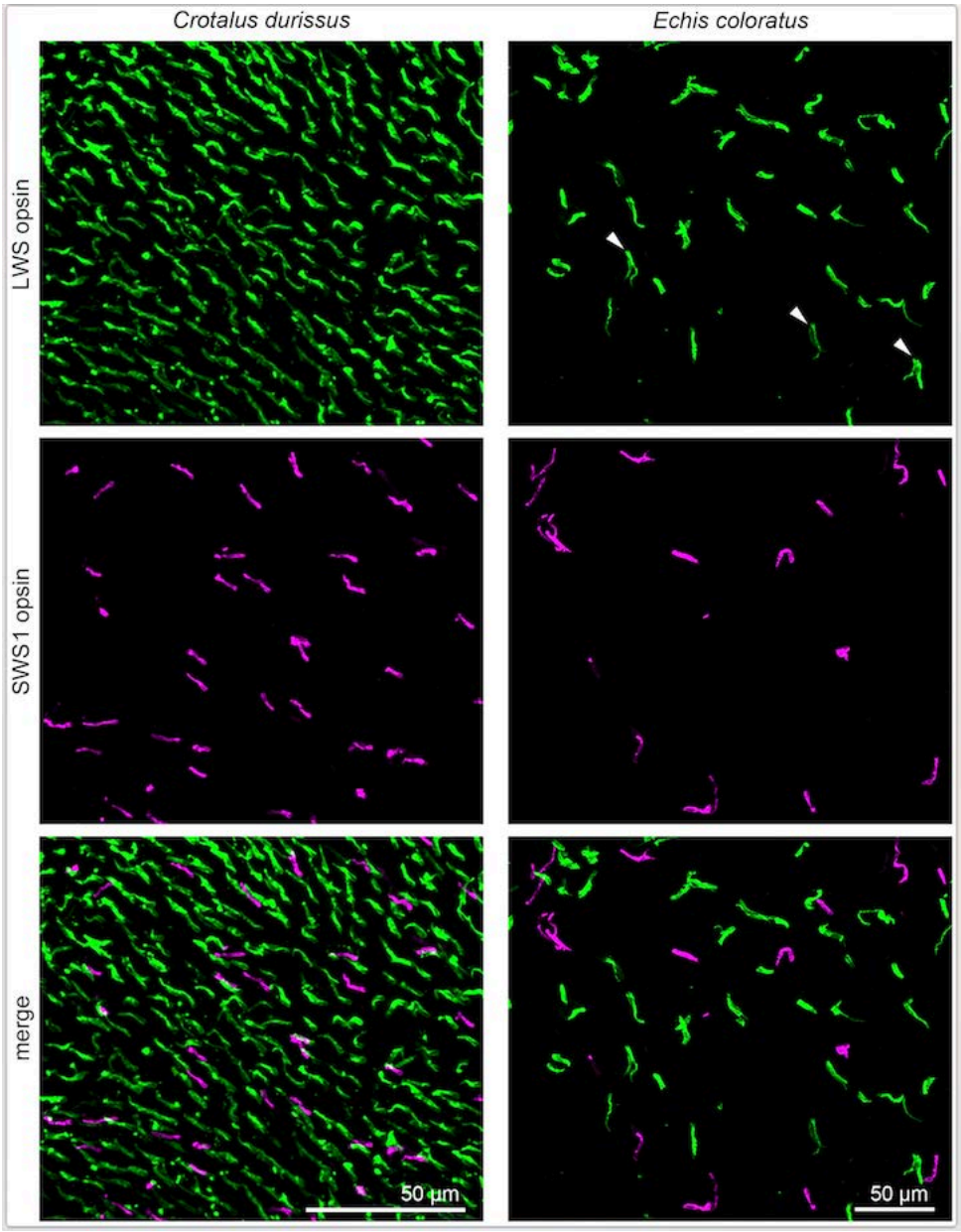
Crotalus durissus
Echis coloratus
LWS opsin
SWS1 opsin
merge
50 µm
50 µm

Fig. 8

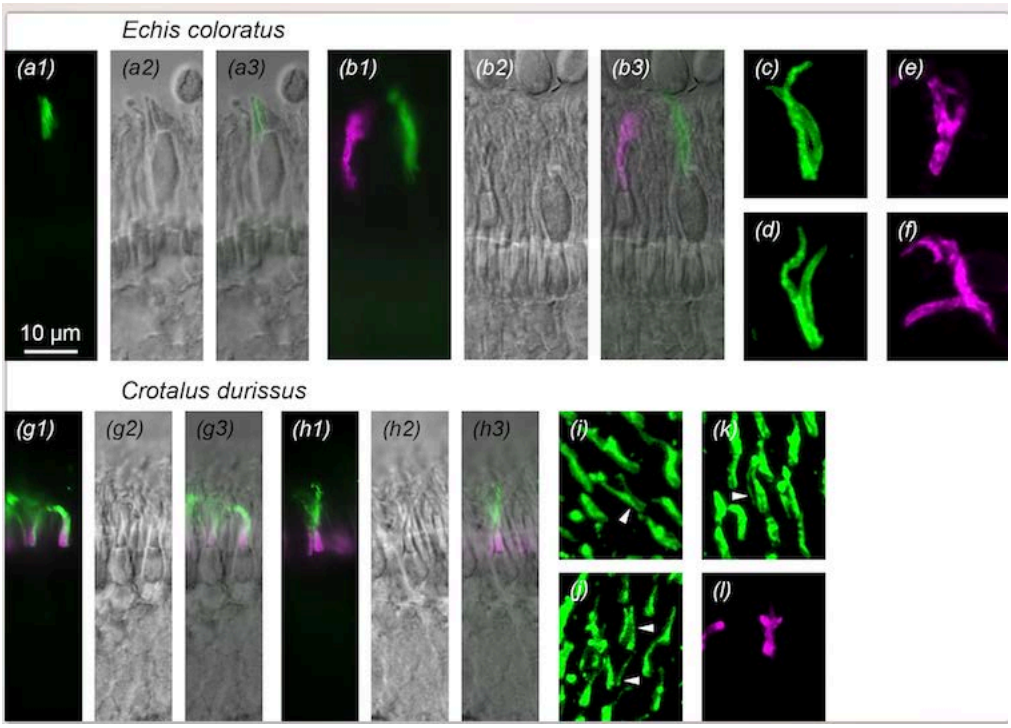
Echis coloratus
(a1)
(a2)
(a3)
(b1)
(b2)
(b3)
(c)
(e)
(d)
(f)
10 µm
Crotalus durissus
(g1)
(g2)
(g3)
(h1)
(h2)
(h3)
(i)
(k)
(j)
(l)

Fig. 9

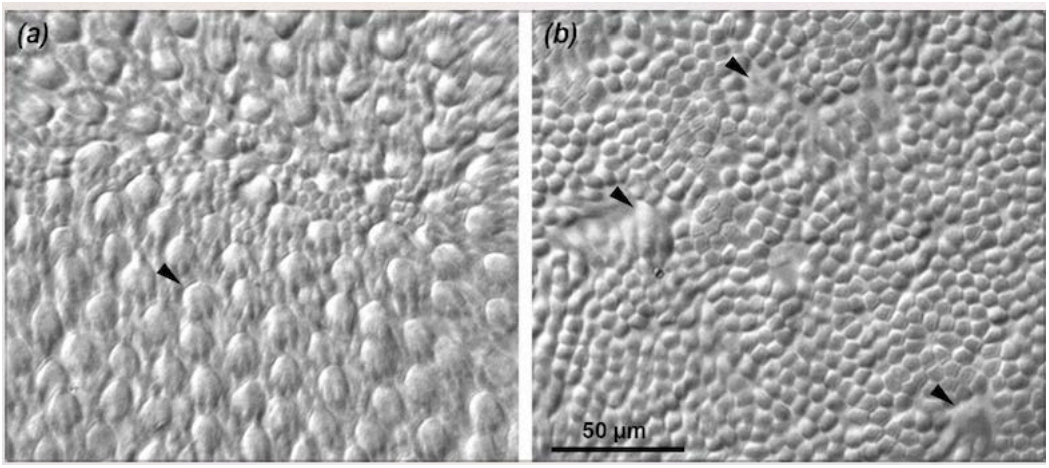
(a)
(b)
50 µm

Fig. 10